DOE/CE/90213--T1

DE89 015147

'3--T1

Annual Report and Program Plan

on

PARTICULATE AND DROPLET DIAGNOSTICS IN SPRAY COMBUSTION

Submitted by

H.G. Semerjian

Chemical Process Metrology Division
Center for Chemical Engineering
National Institute of Standards and Technology
(formerly National Bureau of Standards)
Gaithersburg, MD 20899

Prepared for

Mr. Marvin Gunn
U.S. Department of Energy
Conservation and Renewable Energy
Office of Energy Utilization Research
Energy Conversion and Utilization Technologies Program
Washington, DC 20585

Under Interagency Agreement No. DE-AI01-86CE 90213

November 1986

PARTICULATE AND DROPLET DIAGNOSTICS IN SPRAY COMBUSTION

Hratch G. Semerjian
Center for Chemical Engineering
National Bureau of Standards
Gaithersburg, MD 20899

I. INTRODUCTION

The objective of this project is to investigate droplet evaporation, combustion and particulate formation processes in spray flames, using non-intrusive diagnostic techniques, and to delineate the effect of chemical and physical properties of the fuels on the above processes. The results of this study will provide an experimental data base, with well-defined boundary conditions, for the development and validation of spray combustion models. These models, in turn, can be used to develop computerized design methodologies, to predict combustor performance over a wider range of operating parameters, and to predict the effect of variations in fuel properties on combustion efficiency, radiative energy transfer, and pollutant emissions.

In most combustion systems which utilize liquid fuels, the fuel is introduced into the combustion zone through an atomizer, forming a large number of liquid droplets, which undergo vaporization, mixing (with the oxidizer) and combustion processes. The rate and extent of each of these processes affect overall combustion efficiency, energy transfer and emission of pollutants, such as soot, oxides of nitrogen, CO and unburned

hydrocarbons. Individual droplets transport fuel within the spray and diffuse fuel vapor in their wakes. The rates of vaporization and diffusion are dependent upon the rate of energy transfer by convection and radiation from the flame and its surroundings, as well as the gas phase concentrations surrounding the droplets. It can be seen, then, that the combustion of sprays is a process where mass, momentum and energy transfer and chemical reactions occur simultaneously and are strongly coupled. Our current understanding of spray combustion is not adequate to enable designers of combustion chambers for gas turbines, diesel and direct injection engines, and industrial furnaces and boilers to meet the additional constraints to be imposed by future requirements of fuel flexibility and control of emissions.

Most of the current theoretical analyses have been based on models of single-droplet vaporization with individual droplet burning. These models and droplet combustion studies have been reviewed by Williams [1], Faeth [2,3] and Law [4]. Individual droplet burning may be possible in very dilute sprays with low-volatility fuels; however, recent experimental studies [5-8] have found no evidence of single droplet combustion in laboratory sprays. Indeed, according to Chiu et al. [9], most of the typical industrial oil burners operate at a group combustion number, G, (defined as the ratio of the rate of droplet vaporization to the transport of gaseous species by diffusion) on the order of one or greater, and gas turbine combustors operate at $G > 10$. These correspond to conditions of external group combustion and external sheath combustion regimes, respectively, where the interaction between the droplets cannot be ignored, and the fuel spray and the vapor cloud have to be considered as a whole. More recently, these findings have been substantiated by Yule and Bolado [10], using photographic techniques. As a result of such findings, more recent theoretical efforts

have focused on group combustion or non-dilute spray combustion models [11-16].

Review of the current literature shows that a large portion of experimental efforts has been concentrated on investigation of the combustion of single droplets or arrays of droplets [17-22]. There is a limited amount of information on the detailed structure of spray flames. Most of the studies are focussed on gaseous concentration measurements, with some data on droplets obtained using MgO coated plates [7,8,23,24]. More recent measurements have also been attempted using diffraction techniques [10,25-28], generating qualitative data without any spatial resolution. There are only a limited number of studies, where SPC (single particle counting) techniques have been utilized to obtain detailed, spatially resolved measurements in sprays [29-36]. Based on these observations, it can be concluded that there is a critical need for detailed data on the structure of spray flames, including information on the particle field, droplets, velocity and temperature fields, as well as gaseous species concentrations. The objective of this project is to obtain such a comprehensive data base, as a complementary effort to the spray modelling work being carried out at JPL and LANL. In addition, this study will provide data on the effect of fuel properties and flow field characteristics on the spray combustion processes. Finally, this research effort will focus on identification of the most important sub-processes, such as droplet vaporization, droplet-droplet interactions, droplet-air interactions, radiative energy transfer, etc., which have the greatest impact on the overall characteristics of spray flames.

II. TECHNICAL APPROACH

Experiments are being carried out in a spray combustion facility which simulates operating conditions found in practical combustion systems, and provides flexibility for investigation of flow field and injector geometry effects on combustion characteristics. The spray combustion facility also allows for the study of the effect of fuel properties, including single component as well as multicomponent fuels. A schematic of the variable swirl burner, currently being used for this study, is shown in Fig. 1, and the detailed specifications for the burner are presented in Table 1. This burner design is similar to that used by Beretta et al. [37-39], and will allow for comparison with their experimental results.

A combination of nonintrusive optical diagnostic and intrusive probing techniques are being utilized to obtain comprehensive data on the spray combustion characteristics. A laser velocimetry (LV) system is used to measure the velocity field throughout the combustion region. A dual-beam system is used to measure the axial, radial and tangential velocity components, and the unit is capable of operating in both back scatter and forward scatter configurations. Velocity measurements are obtained from the modulation frequency of the intensity of light scattered by particles traversing the probe volume, formed by the two laser beams. A Bragg cell, operating at 40 MHz, is also utilized to discriminate for velocity direction, which is necessary especially in recirculating parts of the flow. Velocity data are obtained both for the droplets as well as the gas phase, using seed particles, in order to investigate convective effects and the effect of slip on energy and mass transfer processes.

Information on particle and droplet characteristics (diameter, number concentration, volume fraction) is of critical importance, in order to

develop a good understanding of transport processes between the liquid droplets and the gas flow surrounding them. Development of measurement techniques for particle/droplet characterization is an area of intense research, but there are no established experimental techniques that are applicable over the large particle size range (0.01 μm to above 100 μm) and number density range (10^3 - 10^{10} cm^{-3}) required for studies of spray flames. In addition, very few of these techniques have been tested in combustion environments. Therefore, as part of this investigation, several particle diagnostic techniques are being explored and, where possible, results obtained with different techniques are being compared, to establish ranges of applicability, limitations, and the effect of properties such as refractive index and size distribution on measurement accuracy.

Laser based light extinction/scattering (LES) techniques are used to characterize the droplet/particle field in the flame. A typical experimental set-up for these measurements is shown in Fig. 2. Specifically, this apparatus allows measurement of the particle scattering coefficient as a function of laser polarization and scattering angle as well as determining the extinction coefficient. Size and number density measurements can be obtained from ratios of the appropriate scattering coefficients. Specifically, the ratio of scattering to extinction coefficients, the dissymmetry ratios and the polarization ratio are all sensitive to particle size. The first of these ratios is particularly sensitive to small absorbing particles and has been used for soot particle size measurements in the range of .01 to .2 μm, for number densities of 10^{12} to 10^{10} cm^{-3} [40-43]. The dissymmetry ratio yields particle size information for particles of a larger size range, d = 0.1 to 10 μm, for number densities of 10^{10} to 10^5 cm^{-3}. Polarization ratio measurements have been shown to yield information

over a wide range of particle and droplet sizes and appear particularly well suited to high number density conditions ($>10^5$ cm^{-3}) [39,41].

During the past year, the emphasis of our work has been on the measurement of laser scattering polarization ratio, $Q_{hh}(\theta)/ Q_{vv}(\theta)$, in isothermal and combusting sprays. This ensemble scattering/ polarization ratio (ESPR) technique is especially useful in regions of high droplet densities, where single particle techniques will be difficult to apply, and has been demonstrated to provide good discrimination between the presence of soot (or cenosphere) particles and droplets [44-46]. This technique may be an effective method to follow the general trajectory of fuel droplets, to determine the location of the spray ignition zone, and, in conjunction with the LV measurements, the spray ignition times.

In addition to the LES techniques described above, there has been extensive research on sizing techniques involving forward scattering intensity measurements [47,48] and measurements based on analysis of amplitude or phase information from laser velocimetry measurements of particle systems [49-51]. Of the latter group, two approaches have received particular attention: laser visibility (LVV) and phase/Doppler interferometry (PDI) techniques. In the case of the visibility technique (also referred to as the particle sizing interferometry technique), a particle crossing the LV probe volume produces a Gaussian signal (pedestal) with the modulated component superimposed on the pedestal. The ratio of the modulated signal amplitude to the pedestal amplitude provides a measure of particle size as shown by Farmer [49]. This technique is applicable to particles significantly larger than the wavelength of the laser light, and can provide measurements in the diameter range of 1-200 μm. For the phase/Doppler approach, the phase difference between LV measurements made at two different

angles is used to obtain a measure of particle size. An off-axis three-detector version, developed by Bachalo [50,51], has been demonstrated to provide size information for droplets up to 1 mm diameter. Both the visibility and phase/Doppler approaches offer the capability of simultaneous droplet size and velocity measurements. However, both are restricted to single particle scattering and thus are limited to number concentrations of 10^5 cm^{-3} or less.

The laser light scattering intensity deconvolution (LID) technique is another method which involves measurements in the forward scattering direction (small θ) to obtain a measure of the particle size. The intensity of the scattered light generally depends on the location of the particle within the probe volume, as well as on the collection optics configuration. To overcome this problem of non-uniform response within the measurement volume, numerical inversion schemes combined with calibration procedures, have been devised to unfold the distribution of signal amplitudes and provide an indicated size distribution which eliminates the dependence on trajectory [30,31,47,48]. The LID technique can provide particle/droplet sizing capabilities down to about 0.1 μm for number densities extending to 10^5 cm^{-3}.

As mentioned earlier, few comparisons between these various sizing approaches have been carried out [52]. Recently, we have considered several techniques which could provide droplet sizing information for comparison with the polarization ratio results. Of particular interest have been the phase/Doppler and the light intensity deconvolution techniques. Some preliminary results have been obtained and future work will continue in this direction.

The particle/droplet and velocity measurements have been supplemented by intrusive temperature and gas composition measurements, in order to complete the data base needed to characterize the spray combustion process. Temperature measurements are performed using fine-wire thermocouples. Difficulties in obtaining spatially resolved temperature measurements in two-phase flows using this technique are well documented. Recognizing these limitations, the thermocouple results will be used as a qualitative tool to yield relative rather than absolute measurements, especially for comparison between different experiments. Other measurement techniques, currently under development at NBS and elsewhere, will be utilized for this project as they become available. On a limited basis, gas sampling will be used to obtain information on stable gaseous species and particles. Gaseous species, such as CO, CO_2, NO_x, O_2, SO_2 and unburned hydrocarbons can be analyzed on-line with currently available conventional gas analyzers. A more comprehensive gas phase analysis can also be carried out, whenever needed, using a gas chromatograph/mass selective detector (GC/MSD) system.

To summarize, detailed and extensive data will be obtained in a laboratory swirl burner on the combustion characteristics of a spray flame, including data on the spatial distribution of droplet number density, mean drop size and size distribution, droplet and gas velocities, gas temperature and composition, and soot particle size and number density. Experiments will be carried out under a number of conditions, where the flow parameters (air flow velocity, swirl number, inlet air temperature, primary/secondary air split) and fuel injector characteristics (fuel flow rate, spray angle, atomization pressure, atomizer configuration) will be varied over a wide range. These experiments will be utilized to relate the spray combustion characteristics to the critical physical processes, such as fuel-air mixing,

droplet formation and vaporization, flame geometry and recirculation. Experiments carried out with both single component (pentane, heptane, decane) and multicomponent (No. 2 fuel oil, No. 6 fuel oil, and fuels with additives, such as toluene, xylene, napthalene, etc.) fuels will allow elucidation of the relationship between combustion characteristics and fuel properties. Interactions with the parallel modelling efforts being carried out at JPL, LANL and SNLL will provide critical input for this experimental program.

III. PROGRAM PLAN AND STATUS

During the first phase of this project, the design and fabrication of the variable swirl spray burner was completed, and the operating characteristics were evaluated over a wide range of operating conditions. Photography, high speed cinematography, and laser sheet beam scattering techniques were used to identify various regions of the spray flame and to observe trajectories of large droplets and overall features of the flame. These studies have been used to identify: (a) a droplet transport region dominated by the initial momentum of the droplets; (b) an ignition region, controlled by the swirl strength of the air flow; and (c) a combustion plume region, where large scale structures are observed. Some preliminary temperature measurements were also carried out in the spray flame, using fine wire thermocouples.

During the past year, significant progress has been made in several areas. Additional temperature measurements have been obtained in a pressure atomized kerosene spray introduced into the swirling air flow field. Detailed droplet and air velocity measurements were carried out under isothermal and burning conditions, to investigate the effect of energy release on the velocity fields. Droplet and air flow characteristics were determined near the fuel injector and at the exit of the combustion air passage. These measurements have been used as the boundary conditions for the calculations carried out at LANL. Detailed droplet size and number density measurements have been made in isothermal sprays, using the ESPR technique, to investigate the structure of the fuel spray and the effect of swirl on the droplet field. In addition, a comparative evaluation of three droplet sizing techniques (i.e., ESPR, PDI and LID) have been carried out.

Temperature measurements with fine wire thermocouples have been performed to provide information on the nature of the temperature field for comparison with the laser velocimetry and light scattering measurements. Temperature profiles obtained at several heights, with and without the primary air, are shown in Fig. 3. The most striking feature observed in Fig. 3(a) is the presence of two reaction zones in the lower part of the flame. This temperature field is attributed to the independent interaction of the primary and secondary air flows with the fuel spray. The central reaction zone results from the interaction of the primary air flow with the vaporized fuel, transported from the fuel spray cone towards the center of the flame. Thus, it is more typical of a premixed flame and displays a strong blue color. Mixing with the secondary air occurs at the edge of the droplet spray boundary and is more fuel rich. This fact is borne out by the strong yellow luminosity at this region which is due to the presence of soot particles. At higher locations, mixing causes the two high temperature regions to merge and the temperature peak is observed at the center line. Fig. 3(b) shows that, in the absence of the primary air stream, the temperature near the center of the field remains relatively low and unchanged. The central core is now a fuel rich region and the temperature rise is observed only on the edge of the spray cone, where fuel and air mixing occurs. The location of the temperature peak moves radially outward, with increasing axial distance, following the trajectory of the spray sheet.

Complete characterization of the spray flame also requires a detailed knowledge of the droplet and air velocity fields, in order to elucidate the mass and momentum transfer processes in this complex two-phase flow field. Measurements of axial, radial and tangential velocity distributions have been carried out to characterize both the droplet and air flow fields.

Radial profiles of the three droplet velocity components were obtained at several axial positions downstream of the burner nozzle, under both non-swirling and swirling conditions [53,54]. A typical set of results is shown in Figs. 4-7, displaying the effect of swirl and acceleration due to combustion on the droplet velocity fields. Figures 4 and 5 show a progressive decay in both velocity components across the width of the spray, with increasing axial distance. The mean axial and radial velocities are found to reach maxima along the spray sheet where the larger droplets prevail. In the presence of swirling air, the droplet velocity field is significantly modified (compare Figs. 4 and 6). Close to the nozzle, the negative values of U and positive values of V (not shown here) indicate that droplets penetrate through the spray boundary in a radially outward direction and upstream toward the burner. Also to be noted is the increased radial distance over which droplet velocity measurements were recorded in the swirling case. Further downstream of the nozzle exit, mean droplet velocities in the axial and radial direction for the swirling case decay more rapidly, as compared to the nonswirling case, since smaller droplets are entrained and recirculated upstream by the swirling combustion air. Measurements obtained under burning conditions indicate a significant acceleration in the flow at downstream locations (i.e., for Z>15 mm), whereas very small effects are observed near the nozzle (compare Figs. 6 and 7). This is to be expected, since the flame stand-off distance for this case is approximately 20 mm downstream of the nozzle.

Measurements of the three air velocity components were also obtained in order to get a more quantitative understanding of the momentum and mass transport processes controlling the droplet trajectories and evaporation rates, as well as to provide accurate boundary conditions for the numerical

models used to predict the overall flow field. Figures 8-10 show radial profiles of the mean air velocity at several axial locations, in the absence of any droplets. Of particular interest are the radial profiles obtained near the combustion air passage exit (e.g., at Z=10 mm). It can be seen that, in the absence of swirl, a relatively flat axial velocity profile exists across the entire air passage (see Fig. 8). The minimum at the center of the field is due to the presence of the fuel nozzle. When swirl is introduced, the axial velocity profile is distorted substantially and a velocity peak is observed near the outer wall of the air passage (see Fig. 9). The tangential velocity profiles also show a parallel trend. Significant values of the tangential velocity component are measured near the air passage exit, which are not observed in the nonswirling case (see Fig. 10). Because of the complexity of the flow field, accurate boundary conditions are critical for model development and validation.

During the past year, substantial progress was made towards quantitative characterization of the spray droplet field under isothermal and burning conditions. An ensemble light scattering/polarization ratio (ESPR) technique has been employed to determine local fuel droplet characteristics in dense sprays [46]. The technique is based on measurement of the polarization ratio ($\gamma = Q_{hh}/Q_{vv}$) of the scattered light by the droplets. Angular distribution of the polarization ratio, and its sensitivity to refractive index and droplet size, were calculated based on Lorenz-Mie theory; these results were then used to optimize the optical detection scheme. The technique was used to obtain detailed information on the spatial distribution (axial and radial) of the mean droplet size and number density in the spray (see Figs. 11-13). The radial profiles indicate the expected broadening of the spray with increasing axial distance. Again, it

can be seen that the combustion air has a significant effect on the mean droplet size only at downstream regions of the spray, where the effects of swirl are dominant. A gradual increase in D_{32} along the axis and the spray sheet is observed when moving downstream in the axial direction. The swirling case continually indicates a slightly larger value of D_{32} than for S=0. This increase in the mean droplet diameter is attributed to the vaporization (or transport) of the smaller droplets, resulting in a larger mean droplet size further downstream. There is also the possibility of droplet coalescence, caused by the relative velocity that exists between smaller and larger droplets. A theoretical treatment on droplet coalescence has recently been attempted by Greenberg and Tambour [55]; however, their numerical results require experimental verification. The unambiguous establishment of the presence of coalescence, and delineation of the parameters controlling droplet coalescence phenomena will be a major step towards a better understanding of spray combustion phenomena.

The presence of relatively small droplets on the axis and larger ones close to the spray boundary is attributed to the characteristic design of this particular fuel nozzle. The presence of two outer peaks in Fig. 13 also indicates the position of the spray sheet, formed by the hollow cone nozzle. The middle peak results from droplets that are confined to the axis by the primary air (refer to Ref. [53]). The smaller peak measured on the right side of the profiles was initially thought to be an experimental artifact. However, recent photographic evidence has shown that this may be attributed to the spoke-like variation in droplet concentration caused by the nozzle design (see Fig. 14(a)). This structure disappears when swirling combustion air is introduced (see Fig. 14(b)) [56].

To provide for a comparative evaluation of droplet sizing techniques, data were also obtained with the phase/Doppler and the light intensity deconvolution systems under identical experimental conditions [57]. Figure 15 presents radial profiles of mean droplet diameter obtained with the PDI system for the swirling case. The results reveal that the shape of these profiles at all axial positions is similar to those shown in Fig. 12, which were obtained using the ESPR technique. However, the mean droplet size obtained with the PDI system is about 2-3 times larger than that obtained with the ESPR technique. This may be attributed to the relative insensitivity of the polarization ratio to droplets larger than about 60 μm. Figure 16 shows the measured size distributions for several radial positions at Z=25.4 mm under swirling conditions. The results indicate a progressive increase in mean droplet size with radial distance. The presence of a bimodal distribution of droplets at r=15 mm may be attributed to the spoke-like structure of the spray sheet mentioned above. A typical size-velocity correlation obtained near the spray sheet at r=15 mm and Z=25.4 mm is presented in Fig. 17(a). The results show good correlation, with larger size droplets traveling at higher velocities than the smaller counterparts. This correlation is more pronounced in regions of the spray where large droplets are present. Generally, no correlation is obtained when the large droplets are absent; e.g., at r=0 and Z=25.4 mm, see Fig. 17(b).

Data were also recorded using the LID apparatus at several axial and radial locations within the fuel spray. Close to the nozzle exit the droplet number density was beyond the capability of the available optical arrangement; this particular configuration limited the use of the apparatus to only dilute regions of the spray. Typical results taken at r=38.1 mm and Z=76.2 mm under swirling conditions are presented in Fig. 18. The space in

the middle of the distribution results from elimination of the background noise level in each size range. The mean size obtained with this system is much smaller than that obtained with the PDI system and is comparable to that obtained with the ESPR technique. The PDI data presented in Fig. 16 indicate that most droplet sizes are observed to be larger than approximately 2 μm. This would explain the observed difference in the measured value of D_{32} between the ESPR and PDI techniques.

Based on these observations, our work during the coming year will concentrate on the following three areas:

a) Comparative evaluation of droplet sizing techniques: this work will be continued, with an emphasis towards identifying the applicable range of droplet size and number density, and the limitations associated with variations in the droplet refractive index.

b) Investigation of the effect of fuel properties on spray flames: the next sequence of experiments will be carried out with a residual fuel, to obtain some preliminary data in a system of practical interest and to demonstrate the capabilities of the measurement techniques. A more systematic investigation of fuel structure effects will then be carried out with single component fuels (e.g., heptane), kerosene and residual fuels. This sequence will be undertaken after the new air-assist atomizer is installed in the facility (see section (c) below).

c) Investigation of the effect of atomization on spray characteristics: we have modified a research nozzle developed by Parker Hannifin for installation in our facility. This is an air-assist atomizer, typical of those

used in industrial applications, especially for heavy fuels. This nozzle will be used for all future experiments. This will also enable comparison of results with other investigators who are using identical fuel injectors.

These results will provide needed data on the effect of droplet size distribution on the evaporation and reaction rates, and on the coupling with flow field characteristics (inlet air velocity, swirl number, stoichiometry, etc.). The experiments to be carried out with the air-assist atomizer will provide data on the effect of atomization characteristics on the structure of the spray flame. The experiments with different fuels (both single and multicomponent) will provide critically needed information on the effect of physical and chemical characteristics of fuels on droplet vaporization and pyrolysis, combustion, particulate formation, and gaseous pollutant formation processes.

A set of milestones for CY 1987 are presented in Table 2.

References

1. A. Williams; "Fundamentals of Oil Combustion", Prog. Energy & Comb. Sci., Vol. 2, pp. 167-179 (1976).

2. G.M. Faeth; "Current Status of Droplet and Liquid Combustion", Prog. Energy & Comb. Sci., Vol. 3, pp. 191-224 (1977).

3. G.M. Faeth; "Evaporation and Combustion of Sprays", Prog. Energy & Comb. Sci., Vol. 9, pp. 1-76 (1983).

4. C.K. Law; "Recent Advances in Droplet Vaporization and Combustion", Prog. Energy & Comb. Sci., Vol. 8, pp. 169-199 (1982).

5. N.A. Chigier and C.G. McCreath; "Combustion of Droplets in Sprays", Acta Astronautica, Vol. 1, pp. 687-710 (1974).

6. N.A. Chigier, C.G. McCreath and R.W. Makepeace; "Dynamics of Droplets in Burning and Isothermal Kerosene Sprays", Comb. & Flame, Vol. 23, pp. 11-16 (1974).

7. Y. Onuma and M. Ogasawara; "Studies on the Structure of a Spray Combustion Flame", Proc. 15th Symp. (International) on Combustion, pp. 453-463 (1974).

8. Y. Onuma, M. Ogasawara and T. Inoue; "Further Experiments on the Structure of a Spray Combustion Flame", Proc. 16th Symp. (International) on Combustion, pp. 561-567 (1976).

9. H.H. Chiu and T.M. Liu; "Group Combustion of Liquid Droplets", Comb. Sci. & Tech., Vol. 17, pp. 127-142 (1977).

10. A.J. Yule and R. Bolado; "Fuel Spray Burning Regime and Initial Conditions", Comb. & Flame, Vol. 55, pp. 1-12 (1984).

11. H.H. Chiu, H.Y. Kim and E.J. Croke; "Internal Group Combustion of Liquid Droplets", Proc. 19th Symp. (International) on Combustion,, pp. 971-980 (1982).

12. M. Labowsky and D.C. Rosner; "Group Combustion of Droplets in Fuel Clouds: I. Quasi-Steady Predictions", Adv. in Chemistry Series 166, Evaporation-Combustion of Fuels, J.T. Zung, Ed., pp. 63-79 (1978).

13. S.M. Correa and M. Sichel; "The Group Combustion of a Spherical Cloud of Monodisperse Fuel Droplets", Proc. 19th Symp. (International) on Combustion, pp. 981-991 (1982).

14. A.R. Kerstein and C.K. Law; "Percolation in Combustion Sprays I: Transition from Cluster Combustion to Percolate Combustion in Non-Premixed Sprays", Proc. 19th Symp. (International) on Combustion, pp. 961-969 (1982).

15. J. Bellan and R. Cuffel; "A Theory of Non-dilute Spray Evaporation Based Upon Multiple Drop Interactions", Comb. & Flame, Vol. 51, pp. 55-67 (1983).

16. M. Sichel and S. Palaniswamy; "Sheath Combustion of Sprays", Proc. 20th Symp. (International) on Combustion, pp. 1789-1798 (1984).

17. J.J. Sangiovanni and L.G. Dodge; "Observations of Flame Structure in the Combustion of Monodispersed Droplet Streams", Proc. 17th Symp. (International) on Combustion, pp. 455-464 (1978).

18. K. Miyasaka and C.K. Law; "Combustion of Strongly-Interacting Linear Droplet Sprays", Proc. 18th Symp. (International) on Combustion, pp. 283-292 (1980).

19. J.C. Lasheras, A.C. Fernandez-Pello and F.L. Dryer; "On the Disruptive Burning of Free Droplets of Alcohol/n-Paraffin Solutions and Emulsions", Proc. 18th Symp. (International) on Combustion, pp. 293-304 (1980).

20. J.J. Sangiovanni and D.S. Liscinsky; "Soot Formation Characteristics of Well-Defined Spray Flames", Proc. 20th Symp. (International) on Combustion, pp. 1063-1073 (1984).

21. C.P. Koshland and C.T. Bowman; "Combustion of Monodisperse Droplet Clouds in a Reactive Environment", Proc. 20th Symp. (International) on Combustion, pp. 1799-1807 (1984).

22. T.Y. Xiong, C.K. Law and K. Miyasaka; "Interactive Vaporization and Combustion of Binary Droplet Systems", Proc. 20th Symp. (International) on Combustion, pp. 1781-1787 (1984).

23. S.R. Gollahalli and J.D. Lin; "A Comparative Study of the Structure of Burning Sprays of No. 2 and SRC-II Fuel Oils", Comb. & Flame, Vol. 44, pp. 125-135 (1982).

24. S.R. Gollahalli, M.K. Nasrullah and J.H. Bhashi; "Combustion and Emission Characteristics of Burning Sprays of a Residual Oil and Its Emulsions with Water", Comb. & Flame, Vol. 55, pp. 93-103 (1984).

25. A.J. Yule, C. Ah Seng, P.G. Felton, A. Ungut and N.A. Chigier; "A Laser Tomographic Investigation of Liquid Fuel Sprays", Proc. 18th Symp. (International) on Combustion, pp. 1501-1510 (1980).

26. J.M. Tishkoff, D.C. Hammond and A.R. Chraplyvy; "Diagnostic Measurements of Fuel Spray Dispersion", Jl. Fluids Engineering, Vol. 104, pp. 313-317 (1982).

27. L.G. Dodge and C.A. Moses; "Diagnostics for Fuel Sprays as Applied to Emulsified Fuels", Proc. 20th Symp. (International) on Combustion, pp. 1239-1247 (1984).

28. M. Nakayama and T. Arai; "Measurement of Spray Droplet Evaporation Rate Constant by Laser Diffraction", Proc. 20th Symp. (International) on Combustion, pp. 1259-1264 (1984).

29. N.A. Chigier, A. Ungut and A.J. Yule; "Particle Size and Velocity Measurement in Flames by Laser Anemometer", Proc. 17th Symp. (International) on Combustion, pp. 315-323 (1978).

30. Y. Mizutani, H. Kodama and K. Miyasaka; "Doppler-Mie Combination Technique for Determination of Size-Velocity Correlation of Spray Droplets", Comb. & Flame, Vol. 44, pp. 85-95 (1982).

31. D.J. Holve; "In-Situ Optical Particle Sizing Technique", Jl. Energy, Vol. 4, pp. 176-183 (1980).

32. W.D. Bachalo and M.J. Houser; "Spray Drop Size and Velocity Measurements using the Phase/Doppler Particle Analyzer", Proc. International Conf. on Liquid Atomization and Spray Systems (ICLASS-85), pp. VC/2/1-12 (1985).

33. K. Bauckhage; "Simultaneous Measurements of Velocity and Size of Drops in Free-Flow Fluid Spray", Proc. International Conf. on Liquid Atomization and Spray Systems (ICLASS-85), pp. VC/3/1-11 (1985).

34. M.L. Yeoman, D.J. Hemsley, O. Hadded, C.J. Bates; "A Single Particle Optical Counting Instrument for On-line Simultaneous Measurement of Drop Size, Velocity and Concentration in Sprays and Spray Systems", Proc. International Conf. on Liquid Atomization and Spray Systems (ICLASS-85), pp. VC/1/1-13 (1985).

35. V.G. McDonell, C.P. Wood and G.S. Samuelsen; "A Comparison of Spatially-Resolved Drop Size and Drop Velocity Measurements in an Isothermal Chamber and a Swirl-Stabilized Chamber", Paper presented at the 21st Symp. (International) on Combustion, Munich, Germany (Aug. 1986).

36. C.P. Mao, G. Wang, and N. Chigier; "An Experimental Study of Air-Blast Atomizer Spray Flames", paper presented at the 21st Symp. (International) on Combustion, Munich, Germany (Aug. 1986).

37. F. Beretta, A. Cavaliere, A. D'Alessio and C. Noviello; "Visible and U.V. Spectral Emission and Extinction Measurements in Oil Spray Flame", Comb. Sci. & Tech., Vol. 22, pp. 1-15 (1980).

38. F. Beretta, A. Cavaliere, and A. D'Alessio; "Soot and PAH Distributions in Oil Spray Flames, Inferred by Elastic and Inelastic Laser Light Scattering", Proc. 19th Symp. (International) on Combustion, pp. 1359-1367 (1982).

39. F. Beretta, A. Cavaliere and A. D'Alessio; "Ensemble Laser Light Scattering Diagnostics for the Study of Fuel Spray in Isothermal and Burning Conditions", Proc. 20th Symp. (International) on Combustion, pp. 1249-1258 (1984).

40. R.J. Santoro, H.G. Semerjian and R.A. Dobbins; "Soot Particle Measurements in Diffusion Flames", Comb. & Flame, Vol. 51, pp. 203-218 (1983).

41. R.A. Dobbins, R.J. Santoro and H.G. Semerjian; "Interpretation of Optical Measurements of Soot in Flames", in Combustion Diagnostics by Nonintrusive Methods, T.D. McCay, Ed., Prog. Aero. and Astro., Vol. 92, pp. 208-237 (1984).

42. R.J. Santoro and H.G. Semerjian; "Soot Formation in Diffusion Flames: Flow Rate, Fuel Species and Temperature Effects", Proc. 20th Symp. (International) on Combustion, pp. 997-1006 (1984).

43. R.J. Santoro, T.T. Yeh and H.G. Semerjian; "The Transport and Growth of Soot Particles in Laminar Diffusion Flames", in Heat Transfer in Fire and Combustion Systems (ASME HTD-Vol. 45), pp. 57-69 (1985).

44. A. D'Alessio; "Laser Light Scattering and Fluorescence Diagnostics of Rich Flames Produced by Gaseous and Liquid Fuels; in Particulate Carbon Formation During Combustion, D.C. Siegla and G.W. Smith, Eds., pp. 207-259 (1981).

45. F. Beretta, A. Cavaliere and A. D'Alessio; "Drop Size and Concentration in a Spray by Sideward Laser Light Scattering Measurements", Comb. Sci. & Tech., Vol. 36, pp. 19-37 (1984).

46. C. Presser, A.K. Gupta, R.J. Santoro and H.G. Semerjian; "Droplet Size Measurements in a Swirling Kerosene Spray Flame by Laser Light Scattering", Proc. International Conf. on Liquid Atomization and Spray Systems (ICLASS-85), pp. VIIC/2/1-13 (1985).

47. D.J. Holve and K.D. Annen; "Optical Particle Counting, Sizing, and Velocimetry Using Intensity Deconvolution", Optical Engineering, Vol. 23, pp. 591-603 (Sept./Oct. 1984).

48. D.J. Holve; "Scattering-Cross-Section Single Particle Sizing Methods", paper presented at the 5th International Congress on Applications of Lasers and Electro-Optics (ICALEO-86), Arlington, VA (Nov. 1986).

49. W.M. Farmer; "Measurement of Particle Size, Number Density, and Velocity Using a Laser Interferometer", App. Optics, Vol. 11, pp. 2603-2612 (1972).

50. W.D. Bachalo and M.J. Houser; "Phase/Doppler Spray Analyzer for Simultaneous Measurements of Drop Size and Velocity Distributions", Optical Engineering, Vol. 23, pp. 583-590 (Sept./Oct. 1984).

51. W.D. Bachalo; "Interferometric Single Particle Sizing Methods", paper presented at the 5th International Congress on Applications of Lasers and Electro-Optics (ICALEO-86), Arlington, VA (Nov. 1986).

52. L.G. Dodge, D.J. Rhodes, and R.D. Reitz; "Comparison of Drop-Size Measurement Techniques in Fuel Sprays: Malvern Laser-Diffraction and Aerometrics Phase/Doppler", paper presented at the 1986 Meeting of

the Central States Section/The Combustion Institute, NASA Lewis Research Center, (May 1986).

53. C. Presser, A.K. Gupta, R.J. Santoro and H.G. Semerjian; "Velocity and Droplet Size Measurements in a Fuel Spray", paper No. AIAA-86-0297, presented at the AIAA 24th Aerospace Sciences Meeting, Reno, NV (Jan. 1987).

54. C. Presser, A.K. Gupta, H.G. Semerjian and R.J. Santoro; "Droplet/Air Interaction in a Swirl-Stabilized Spray Flame", to be presented at the 2nd ASME/JSME Thermal Engineering Joint Conf., Honolulu, HI (March 1987).

55. J.B. Greenberg and Y. Tambour; "Far-Field Coalescence Effects in Polydisperse Spray Diffusion Flames", paper presented at the 21st Symp. (International) on Combustion, Munich, Germay (Aug. 1986).

56. C. Presser, A.K. Gupta, R.J. Santoro and H.G. Semerjian; "Effect of Combustion Air Swirl on Liquid Fuel Spray Characteristics", poster paper presented at the 21st Symp. (International) on Combustion, Munich, Germany, (Aug. 1986).

57. C. Presser, A.K. Gupta, R.J. Santoro and H.G. Semerjian; "Laser Diagnostics for Characterization of Fuel Sprays", paper presented at the 5th International Congress on Applications of Lasers and Electro-Optics (ICALEO-86), Arlington, VA (Nov. 1986).

Table 1

Specifications for the Movable-Vane Swirl Burner

Property	Specification	Units
Fuel	No. 2 fuel oil	
Inlet Temperature	25	°C
Max. Oil Flow Rate	6	Kgm/hr
Max. Primary Air Flow Rate	9	Kgm/hr
Max. Secondary Air Flow Rate	87	Kgm/hr
Inlet Air Density	1.185	Kgm/m^3
Energy Throughput	71.8	KW
Stoich. Fuel/Air Ratio	0.0686	
Heating Value	10,310	Kcal/Kgm
Primary Air Passageway Dia.	0.032	m
Secondary Air Passageway Dia.	0.101	m
Swirl Vane Angle (Max.)	70	deg
Number of Vanes	12	
Vane Thickness	0.003	m
Vane Height	0.051	m
Vane Length	0.076	m
Swirl Number (Max.)	0.94	

Table 2

Milestones

1.	Obtain preliminary data on droplet size, number density and velocity in residual fuel flames	Mar. 87
2.	Complete data set (V, T, N, D) for kerosene and heptane spray with air-assist atomizer	July 87
3.	Complete comparative evaluation of ESPR, PDI and LID systems for droplet characterization	Dec. 87

Figure Captions

1. Schematic of the moveable-vane swirl burner.

2. Experimental apparatus for laser scattering measurements.

3. Radial temperature distributions at several heights in the flame, a) with, and b) without primary air.

4. Variation of axial mean droplet velocity with radial position, measured at different axial positions for the isothermal spray under nonswirling conditions.

5. Variation of radial mean droplet velocity with radial position, measured at different axial positions for the isothermal spray under nonswirling conditions.

6. Variation of axial mean droplet velocity with radial position, measured at different axial positions for the isothermal spray under swirling conditions.

7. Variation of axial mean droplet velocity with radial position, measured at different axial positions for the burning spray under swirling conditions.

8. Variation of axial mean combustion air velocity with radial position, measured at different axial positions under nonswirling conditions.

9. Variation of axial mean combustion air velocity with radial position, measured at different axial positions under swirling conditions.

10. Variation of tangential mean combustion air velocity with radial position, measured at different axial positions under swirling conditions.

11. Variation of Sauter mean diameter with radial position, measured at different axial positions under nonswirling conditions.

12. Variation of Sauter mean diameter with radial position, measured at different axial positions under swirling conditions.

13. Variation of number density with radial position, measured at different axial positions under nonswirling conditions.

14. Horizontal cross section of the fuel spray at Z = 76.2 mm under a) nonswirling, and b) swirling conditions.

15. Variation of Sauter mean diameter with radial position, measured at different axial positions under swirling conditions with the phase/Doppler system.

16. Droplet size distribution for several radial positions at Z = 25.4 mm under swirling conditions with the phase/Doppler system.

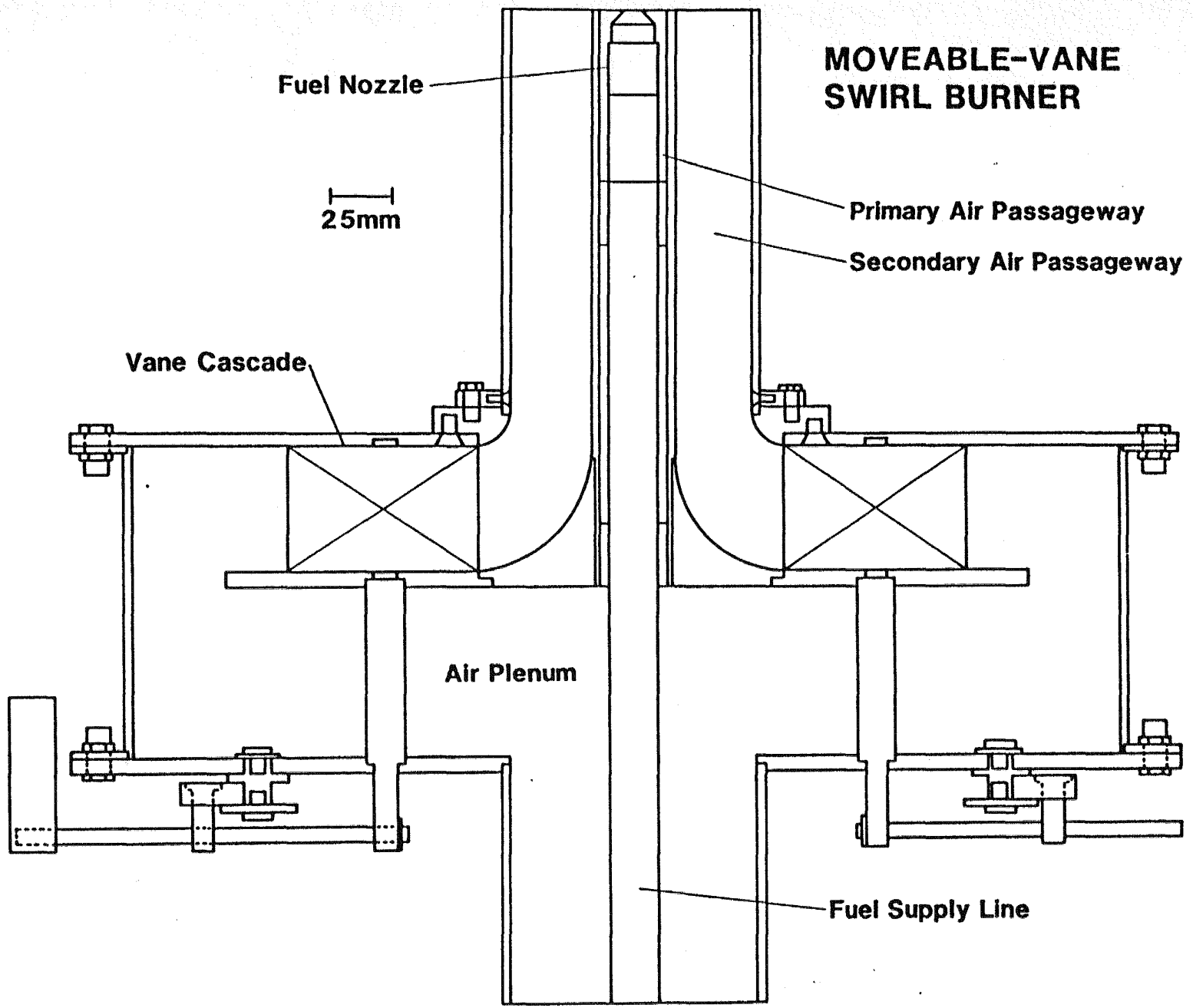
MOVEABLE-VANE
SWIRL BURNER
Fuel Nozzle
25mm
Primary Air Passageway
Secondary Air Passageway
Vane Cascade
Air Plenum
Fuel Supply Line

FIGURE 1

EXPERIMENTAL DROPLET VELOCITY/SIZING APPARATUS

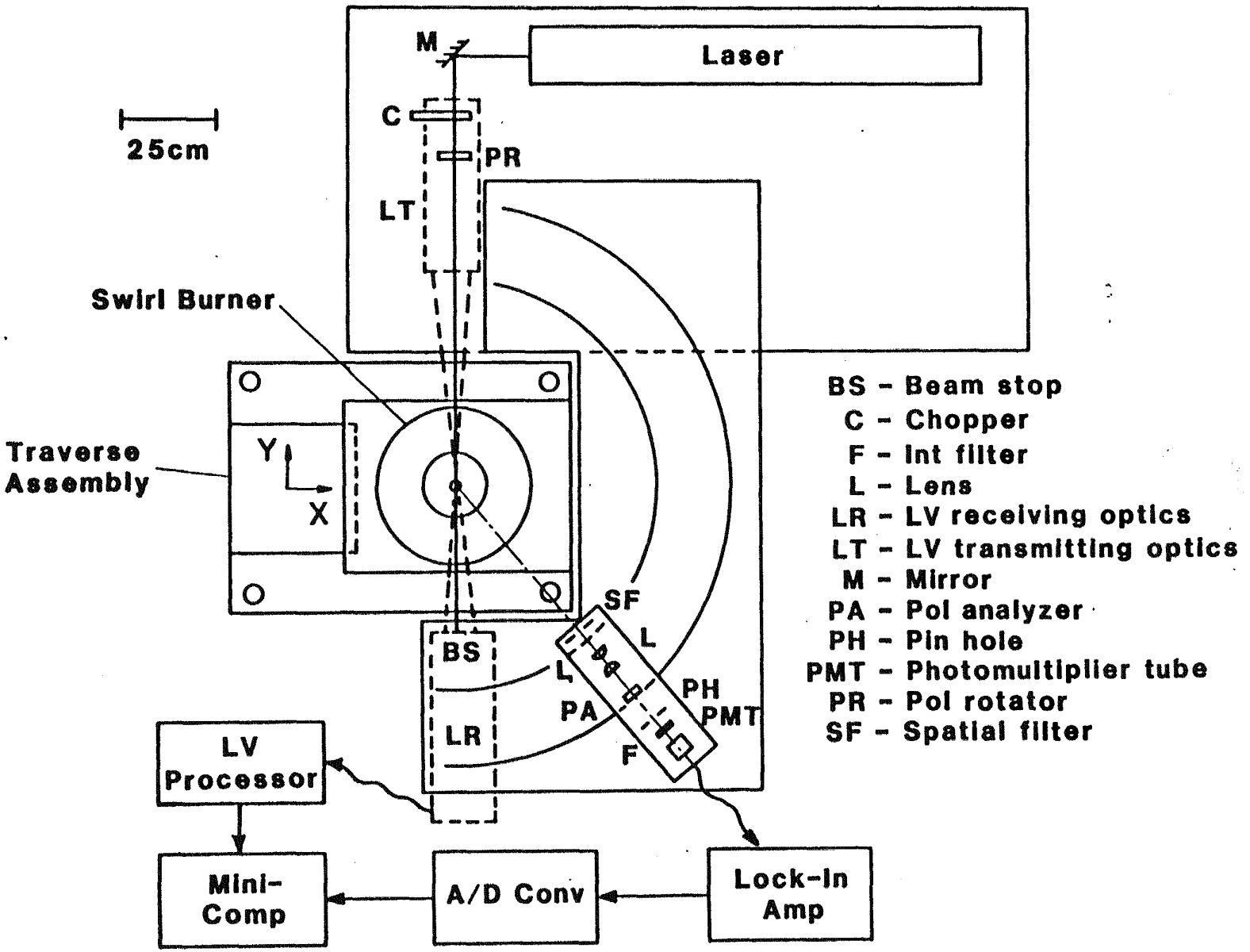

FIGURE 2

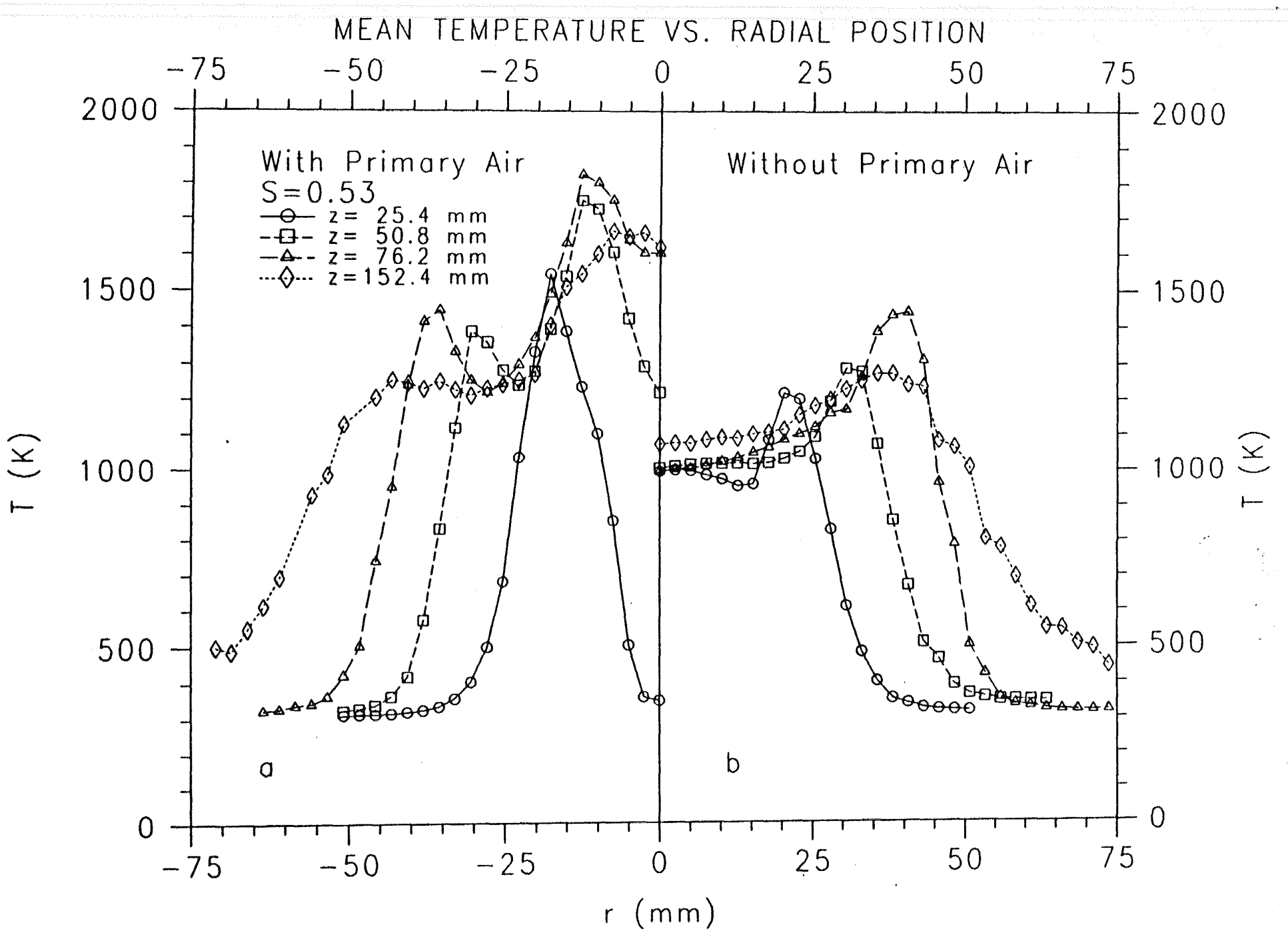
MEAN TEMPERATURE VS. RADIAL POSITION
With Primary Air
S=0.53
z= 25.4 mm
z= 50.8 mm
z= 76.2 mm
z=152.4 mm
Without Primary Air
a
b
T (K)
r (mm)
2000
1500
1000
500
0
-75
-50
-25
0
25
50
75

FIGURE 3

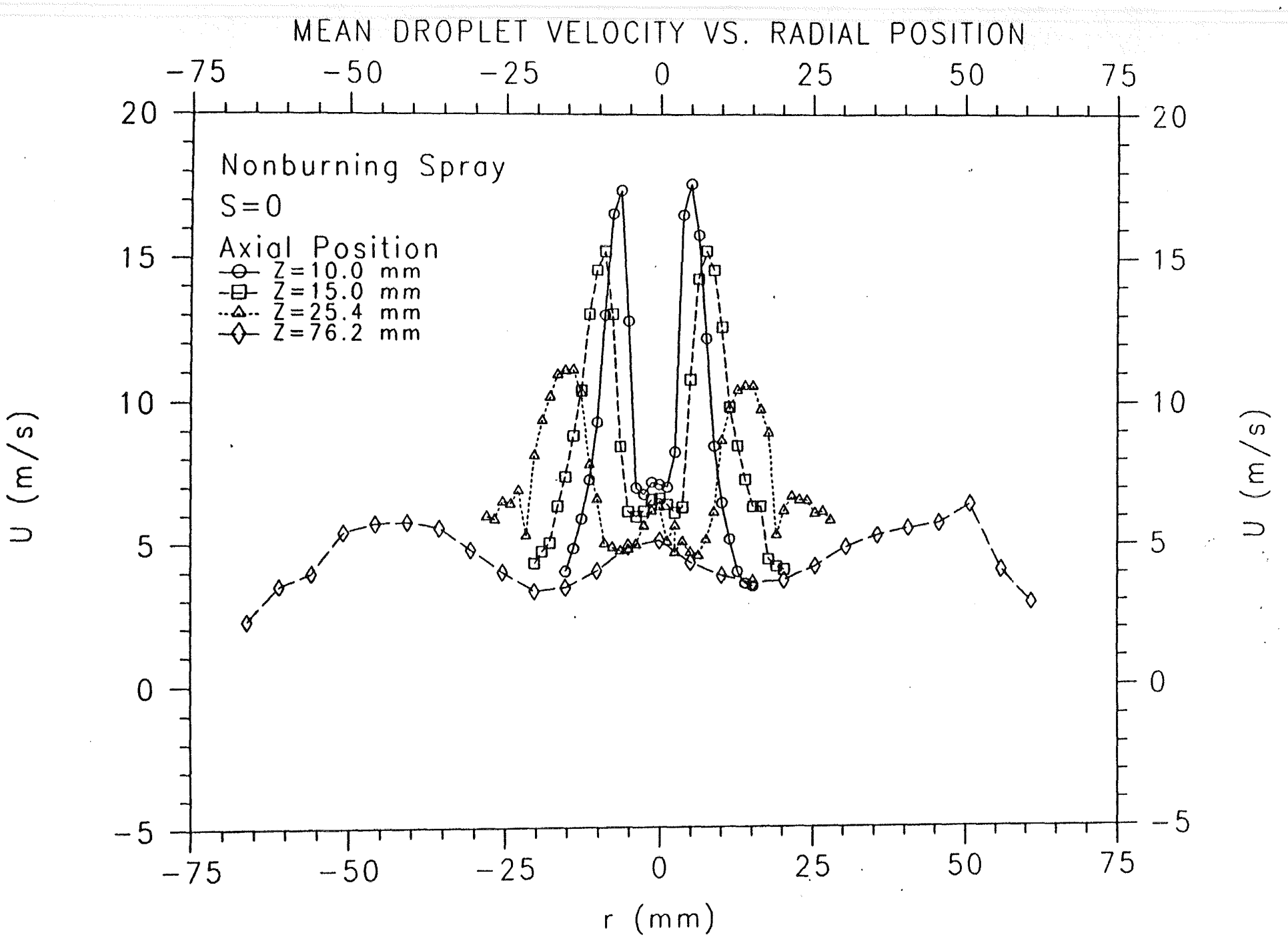
MEAN DROPLET VELOCITY VS. RADIAL POSITION
Nonburning Spray
S=0
Axial Position
Z=10.0 mm
Z=15.0 mm
Z=25.4 mm
Z=76.2 mm
U (m/s)
r (mm)
-75
-50
-25
0
25
50
75
20
15
10
5
0
-5

FIGURE 4

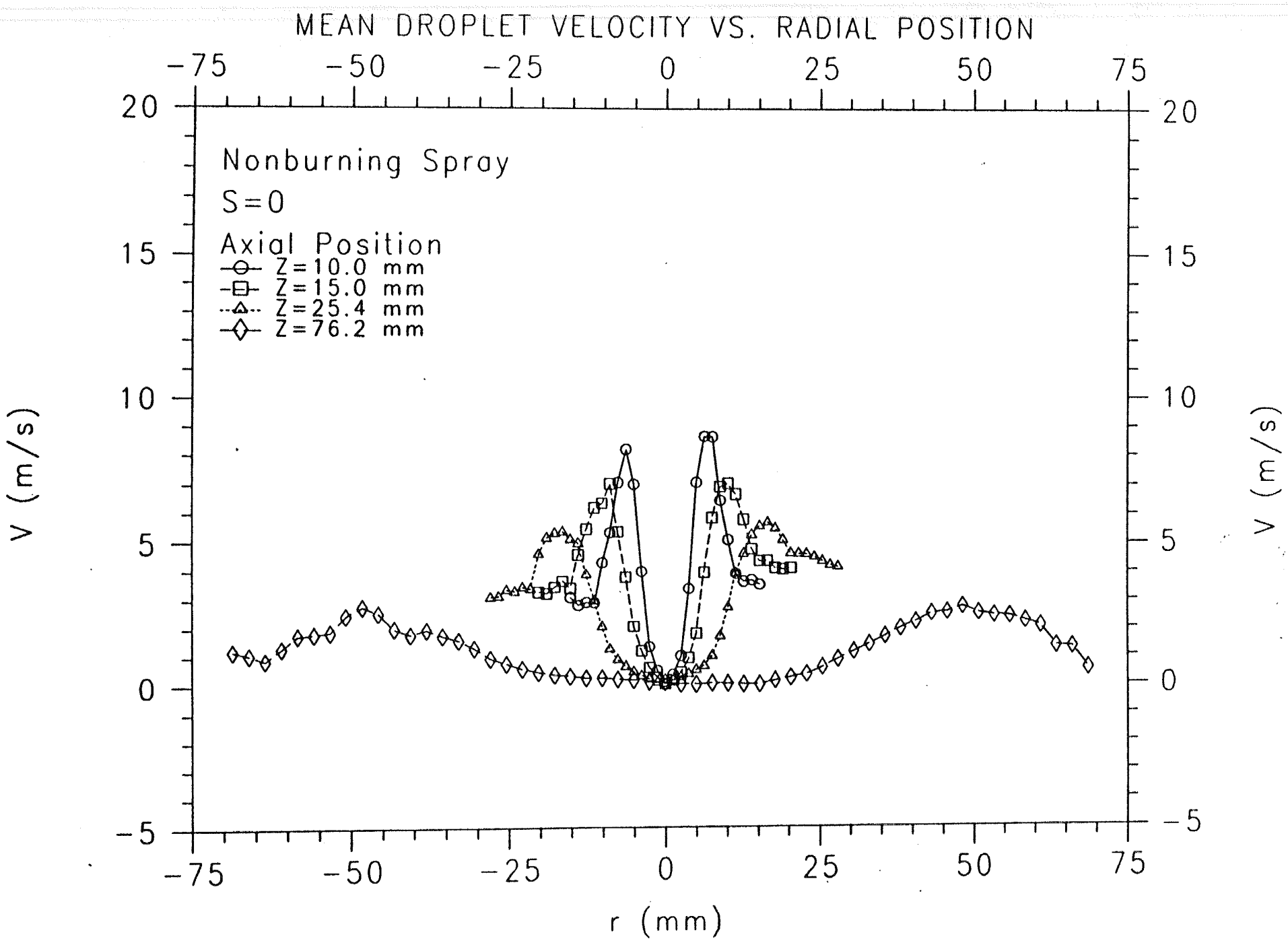
MEAN DROPLET VELOCITY VS. RADIAL POSITION
Nonburning Spray
S=0
Axial Position
Z=10.0 mm
Z=15.0 mm
Z=25.4 mm
Z=76.2 mm
V (m/s)
r (mm)
-75
-50
-25
0
25
50
75
20
15
10
5
0
-5

FIGURE 5

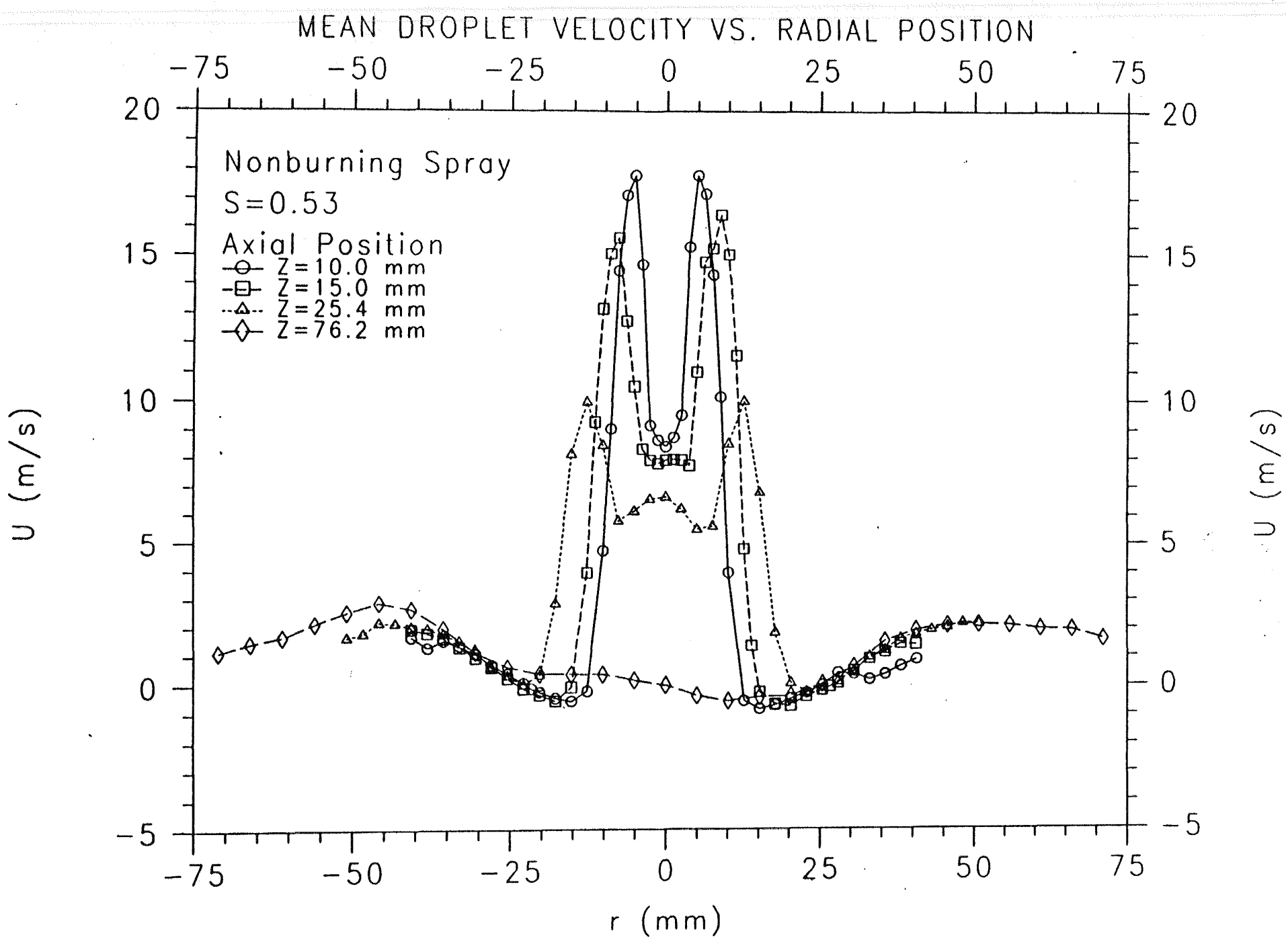
MEAN DROPLET VELOCITY VS. RADIAL POSITION
Nonburning Spray
S=0.53
Axial Position
Z=10.0 mm
Z=15.0 mm
Z=25.4 mm
Z=76.2 mm
U (m/s)
r (mm)
-75
-50
-25
0
25
50
75
20
15
10
5
0
-5

FIGURE 6

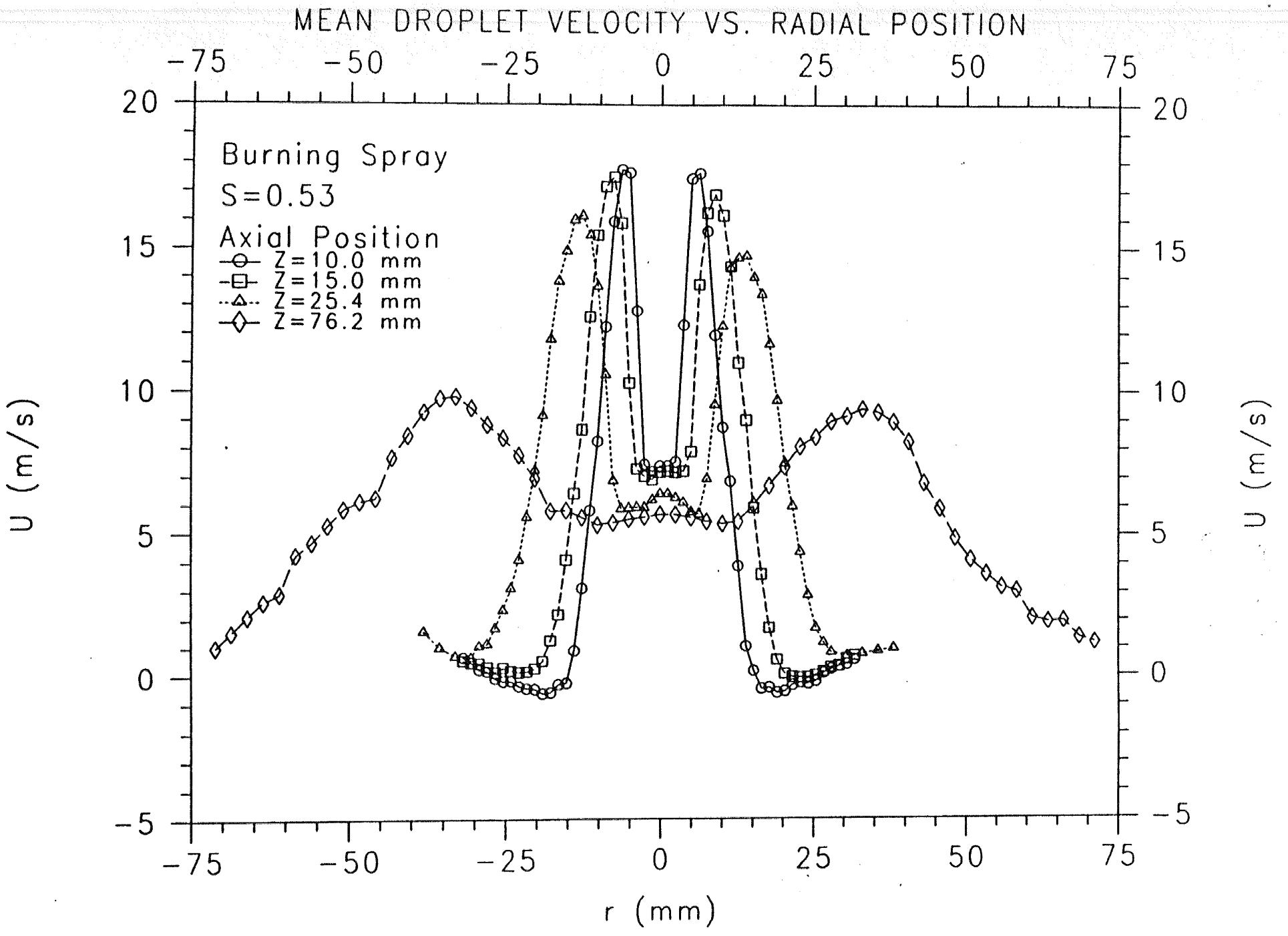
MEAN DROPLET VELOCITY VS. RADIAL POSITION
Burning Spray
S=0.53
Axial Position
Z=10.0 mm
Z=15.0 mm
Z=25.4 mm
Z=76.2 mm
U (m/s)
r (mm)
-75
-50
-25
0
25
50
75
20
15
10
5
0
-5

FIGURE 7

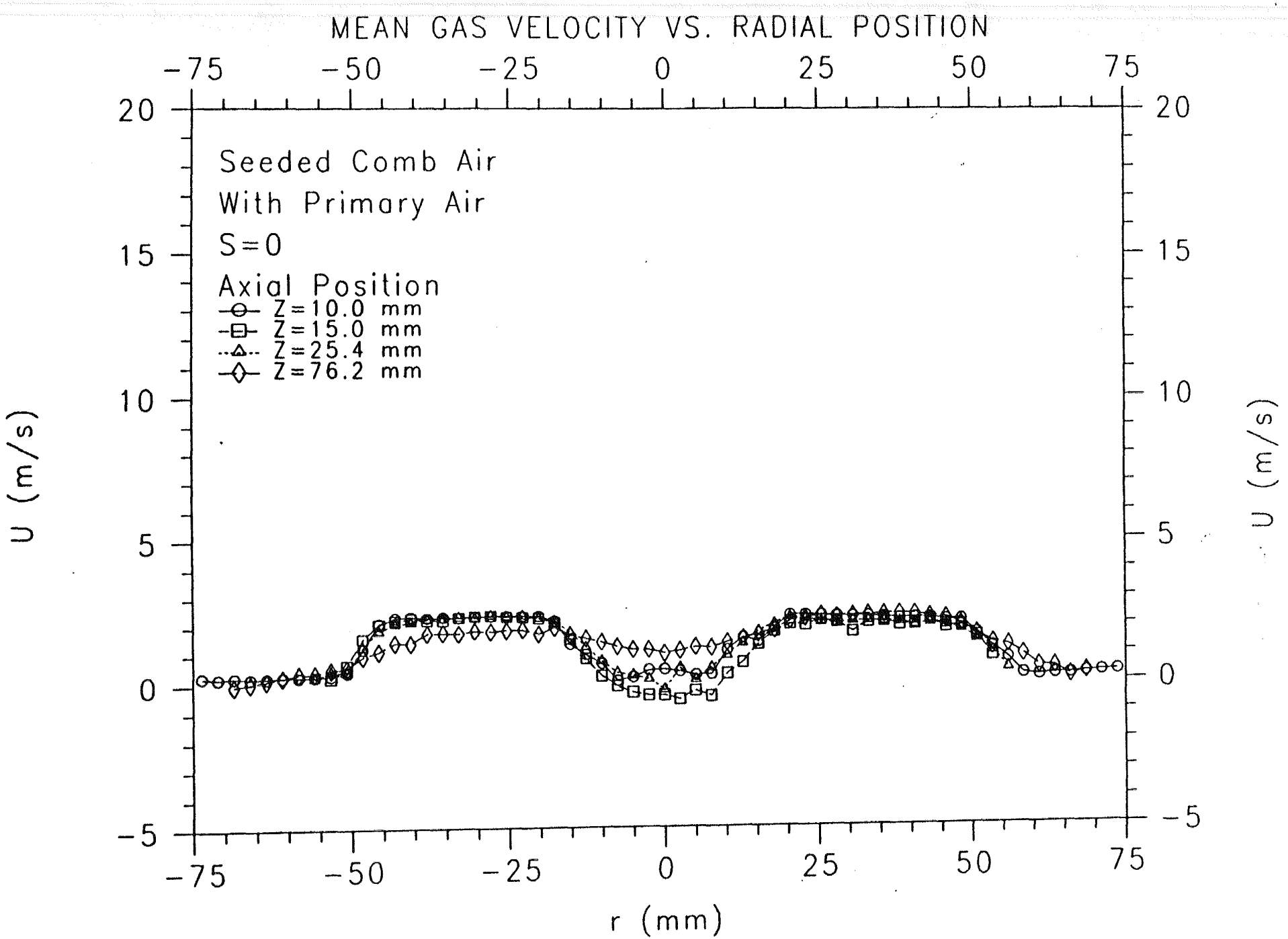
MEAN GAS VELOCITY VS. RADIAL POSITION
Seeded Comb Air
With Primary Air
S=0
Axial Position
Z=10.0 mm
Z=15.0 mm
Z=25.4 mm
Z=76.2 mm
U (m/s)
r (mm)
-75
-50
-25
0
25
50
75
20
15
10
5
0
-5

FIGURE 8

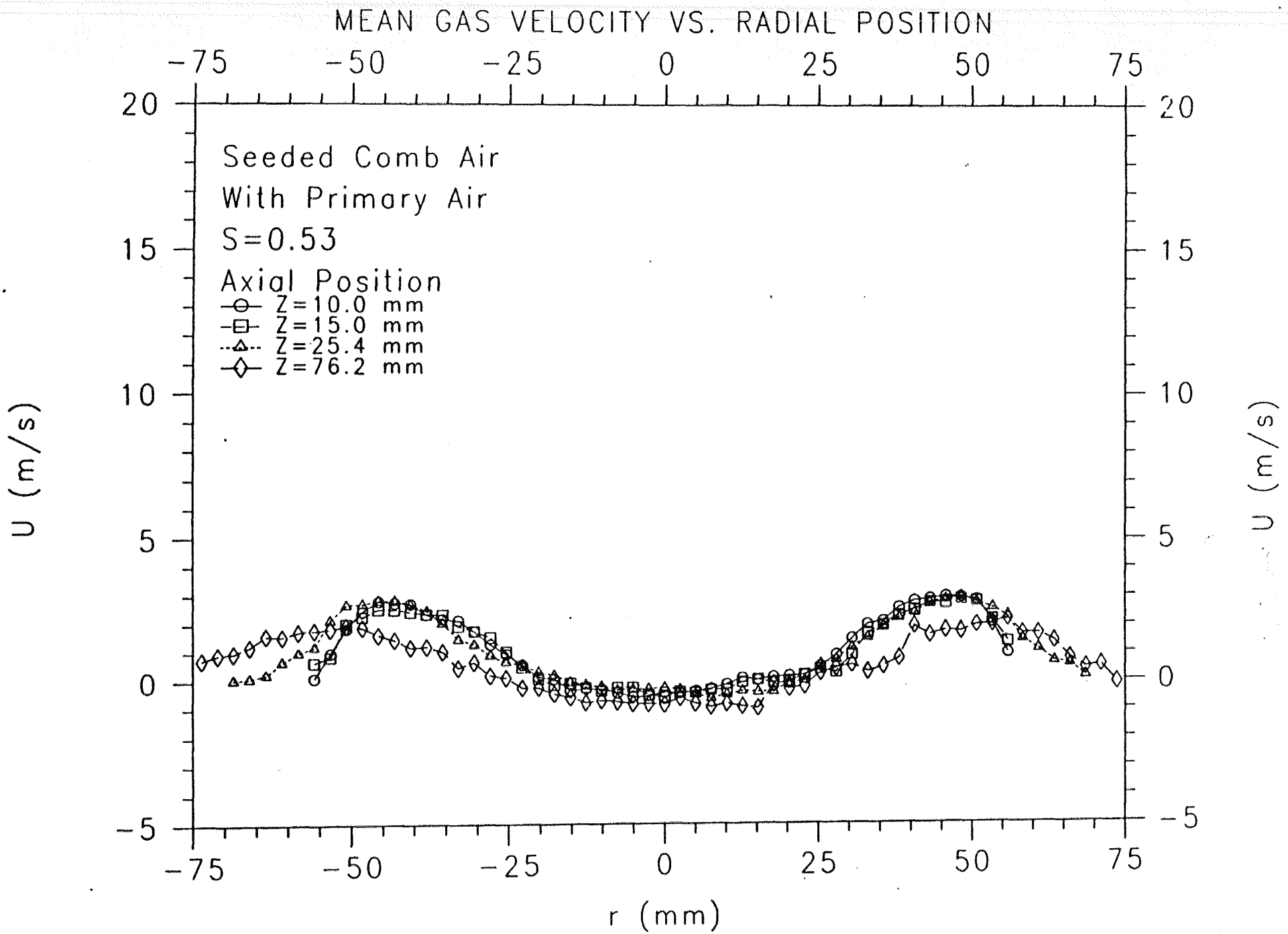
MEAN GAS VELOCITY VS. RADIAL POSITION
Seeded Comb Air
With Primary Air
S=0.53
Axial Position
Z=10.0 mm
Z=15.0 mm
Z=25.4 mm
Z=76.2 mm
U (m/s)
r (mm)
-75
-50
-25
0
25
50
75
20
15
10
5
0
-5

FIGURE 9

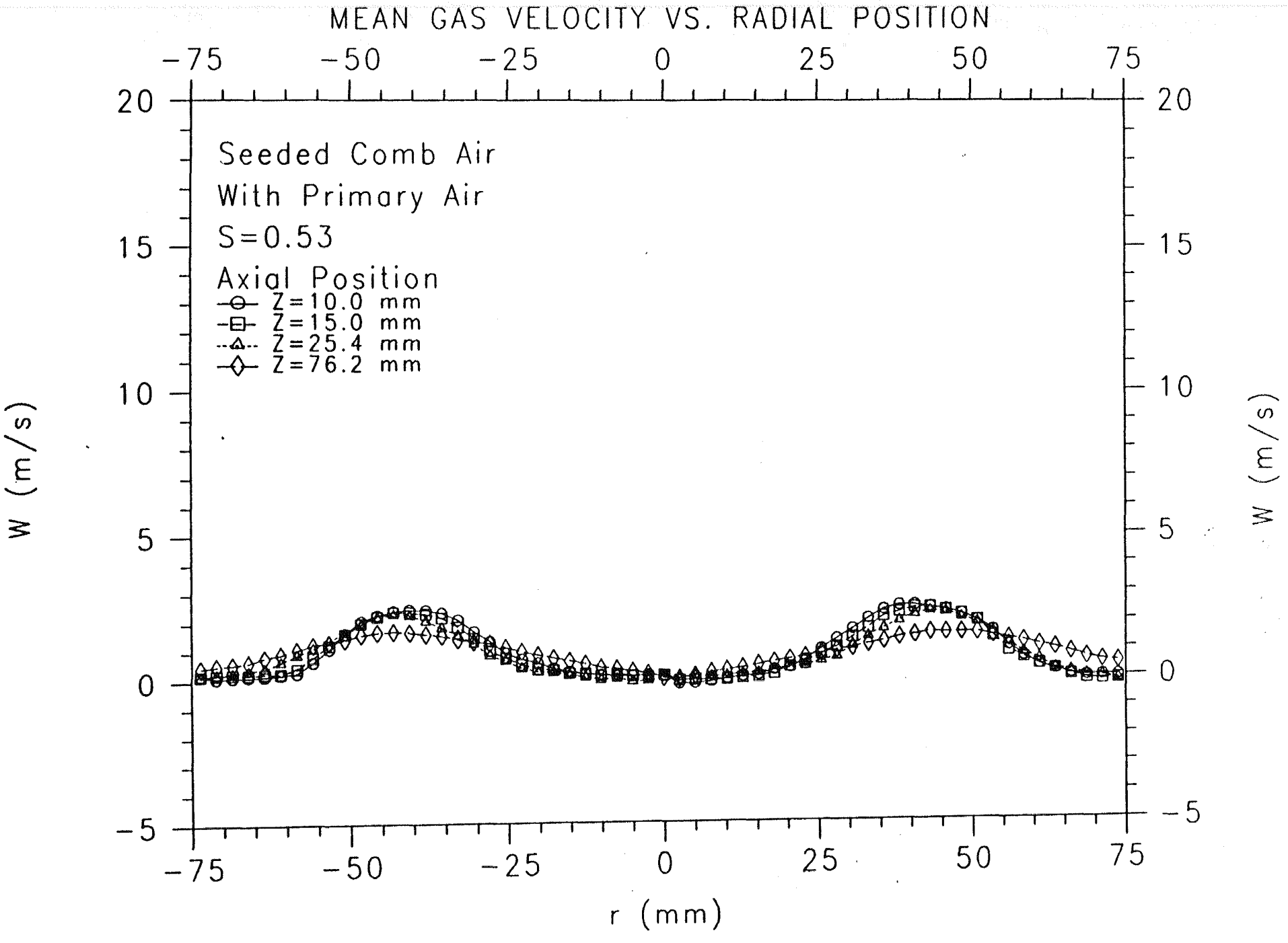
MEAN GAS VELOCITY VS. RADIAL POSITION
Seeded Comb Air
With Primary Air
S=0.53
Axial Position
Z=10.0 mm
Z=15.0 mm
Z=25.4 mm
Z=76.2 mm
W (m/s)
r (mm)
-75
-50
-25
0
25
50
75
20
15
10
5
0
-5

FIGURE 10

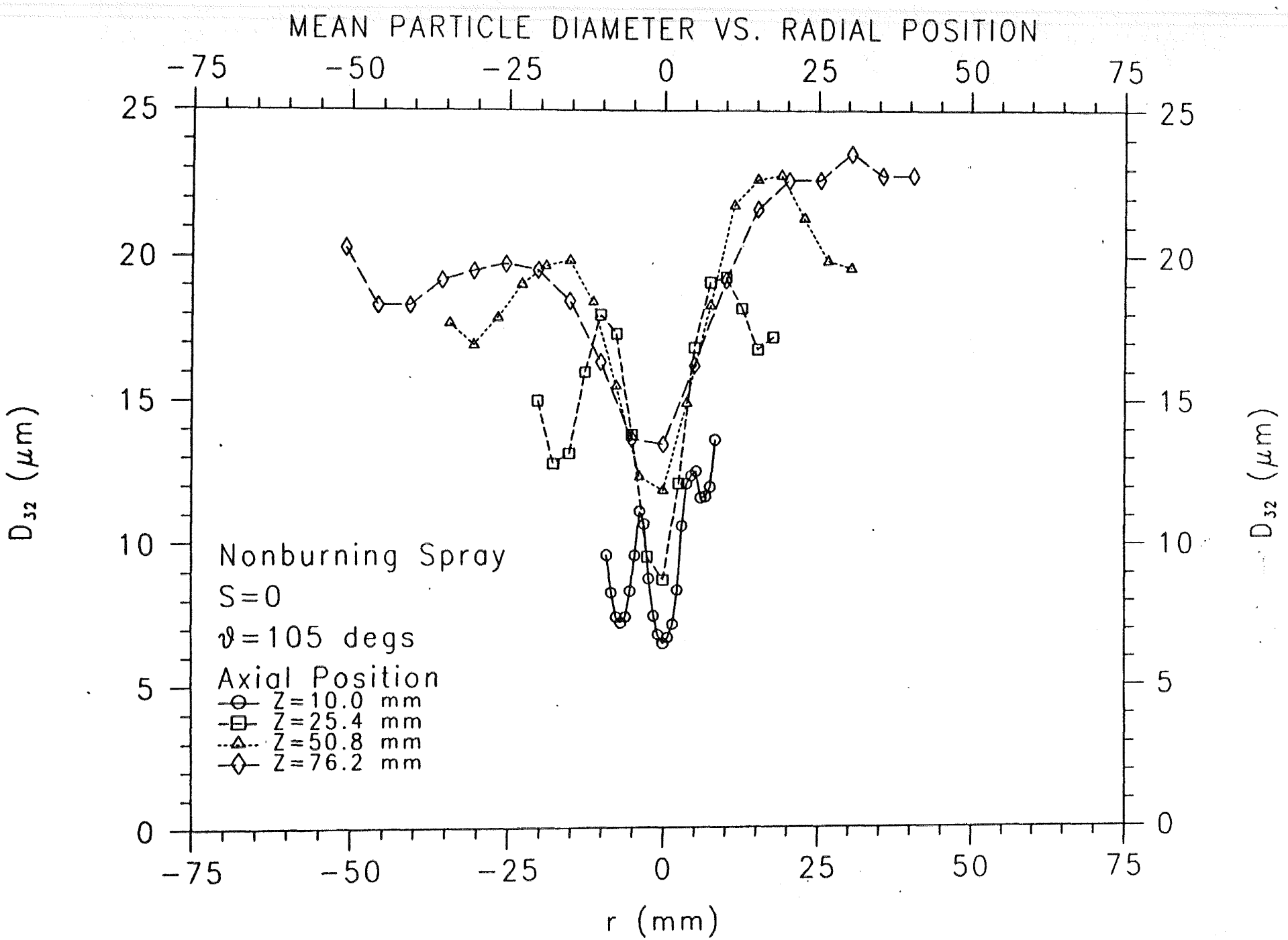
MEAN PARTICLE DIAMETER VS. RADIAL POSITION
-75
-50
-25
0
25
50
75
25
20
15
10
5
0
D_{32} (μm)
Nonburning Spray
S=0
ϑ=105 degs
Axial Position
Z=10.0 mm
Z=25.4 mm
Z=50.8 mm
Z=76.2 mm
r (mm)

FIGURE 11

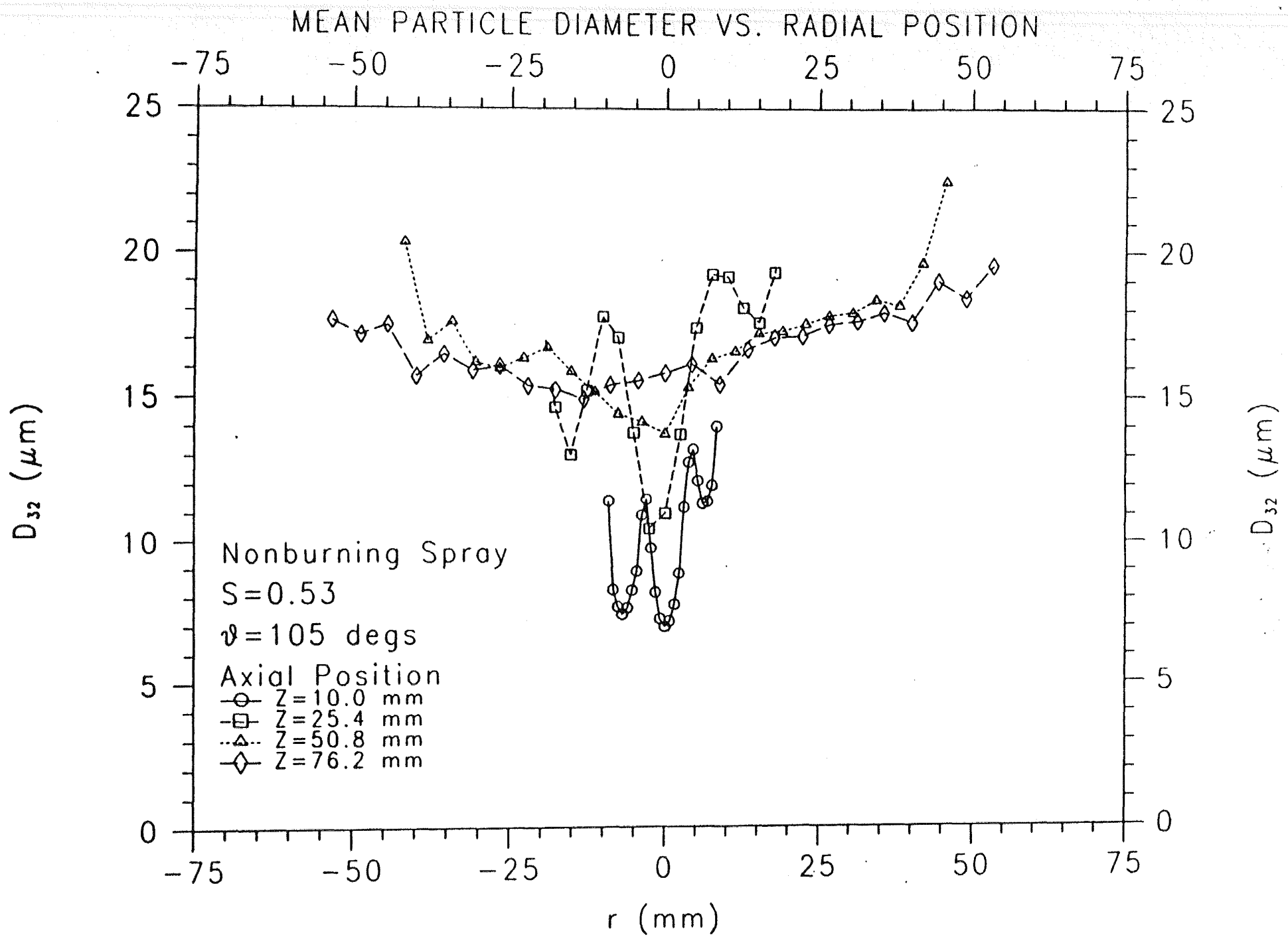
MEAN PARTICLE DIAMETER VS. RADIAL POSITION
-75
-50
-25
0
25
50
75
25
20
15
10
5
0
D_{32} (μm)
Nonburning Spray
S=0.53
ϑ=105 degs
Axial Position
Z=10.0 mm
Z=25.4 mm
Z=50.8 mm
Z=76.2 mm
r (mm)

FIGURE 12

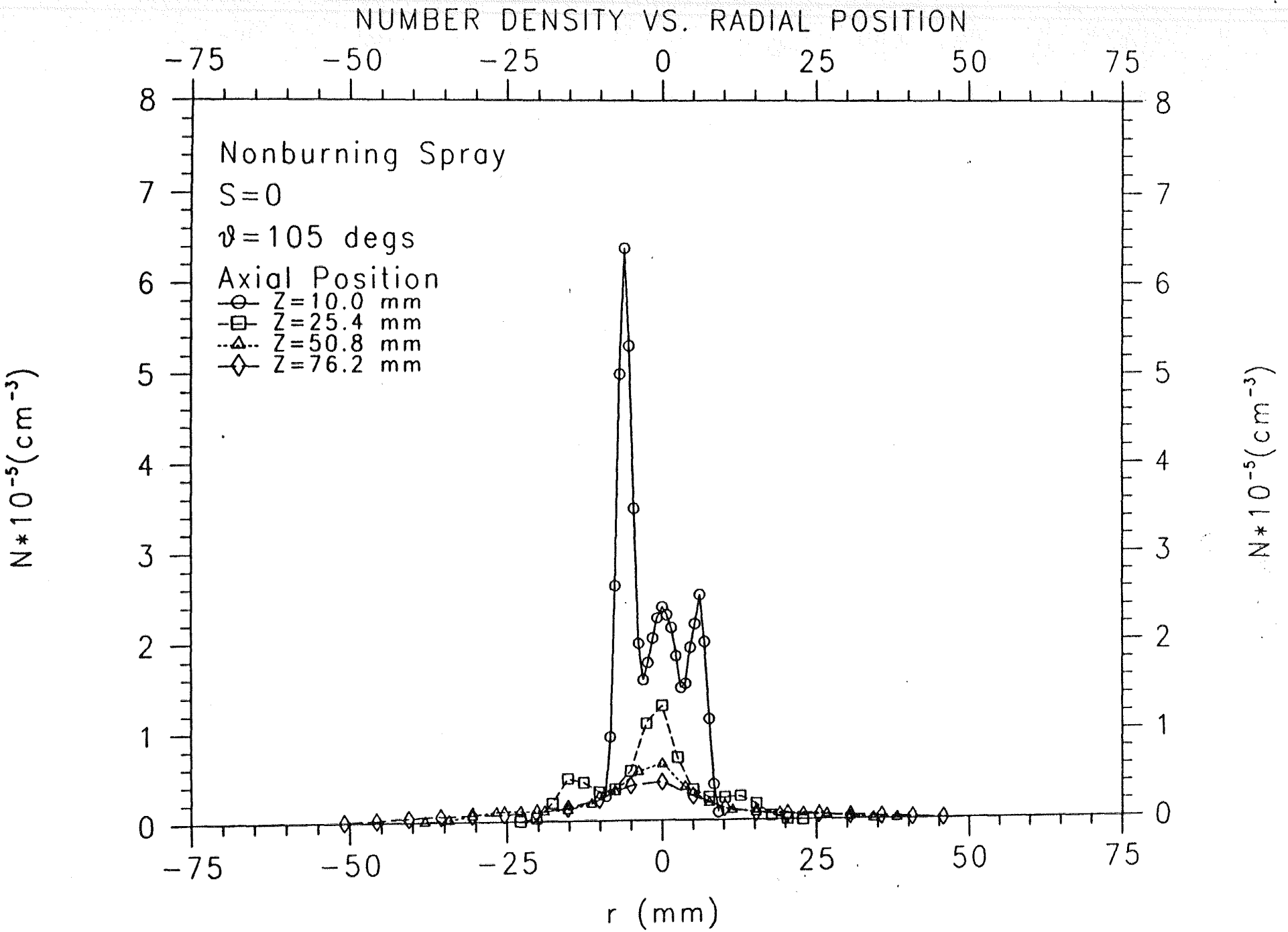
NUMBER DENSITY VS. RADIAL POSITION
Nonburning Spray
S=0
ϑ=105 degs
Axial Position
Z=10.0 mm
Z=25.4 mm
Z=50.8 mm
Z=76.2 mm
N*10^-5(cm^-3)
r (mm)
-75
-50
-25
0
25
50
75
0
1
2
3
4
5
6
7
8

FIGURE 13

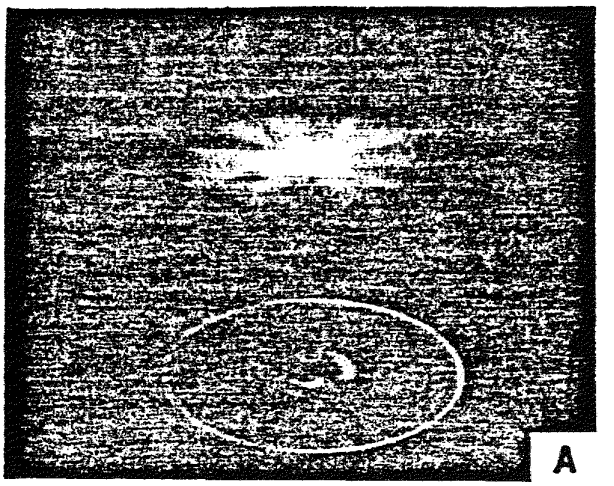

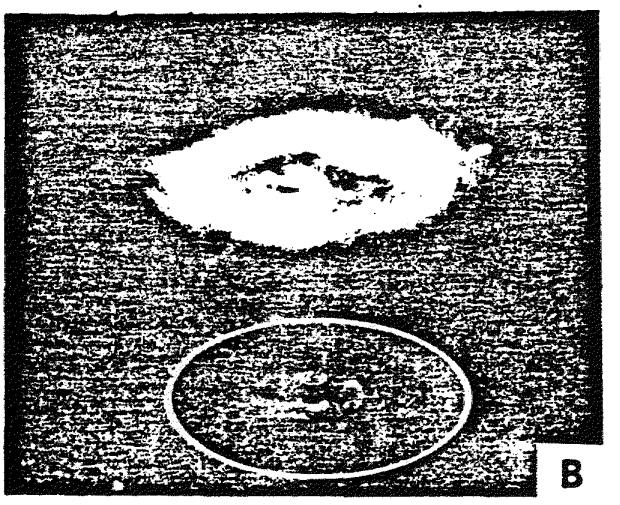

FIGURE 14

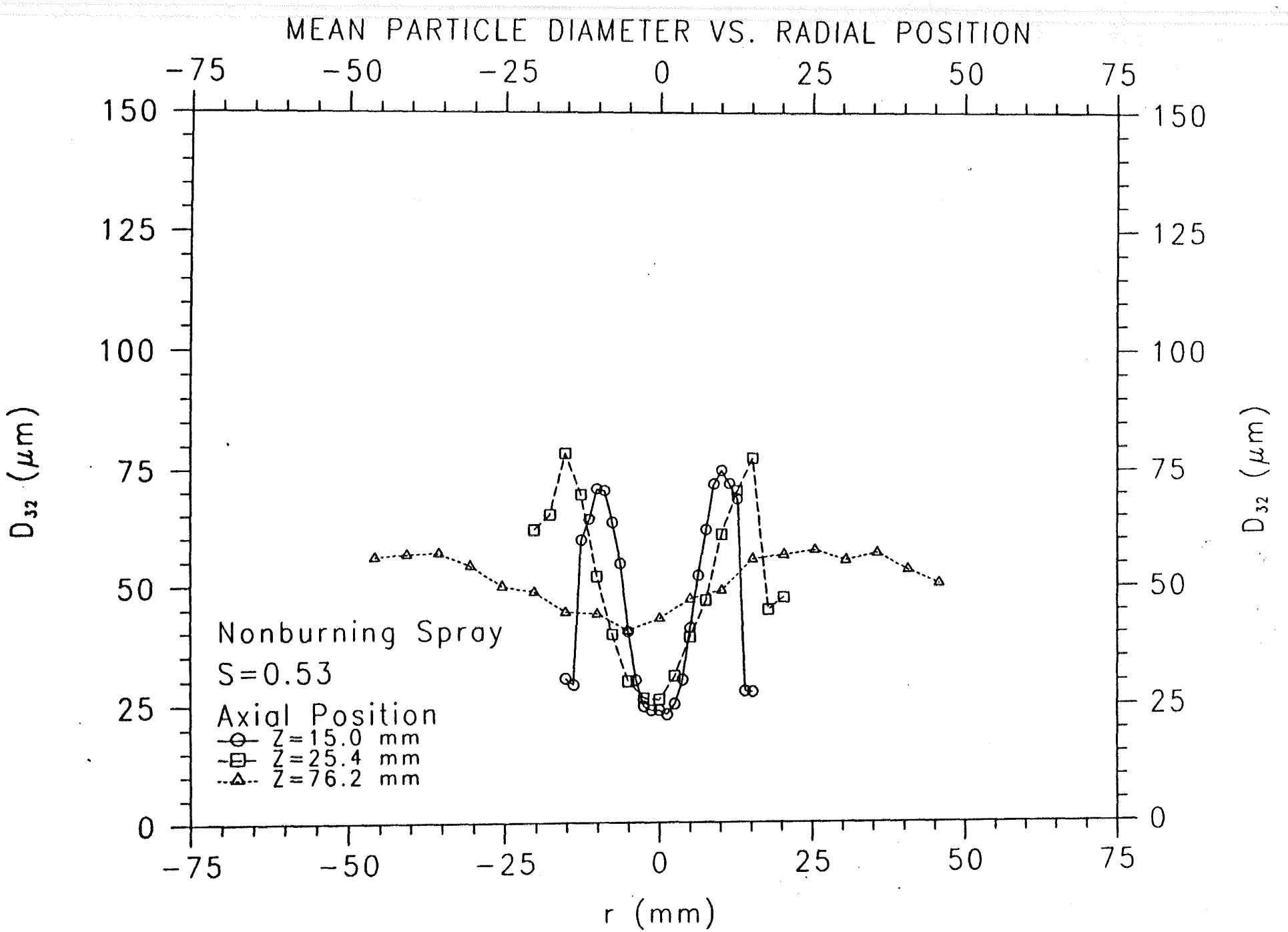
MEAN PARTICLE DIAMETER VS. RADIAL POSITION
−75
−50
−25
0
25
50
75
150
125
100
75
50
25
0
D32 (μm)
Nonburning Spray
S=0.53
Axial Position
Z=15.0 mm
Z=25.4 mm
Z=76.2 mm
r (mm)

FIGURE 15

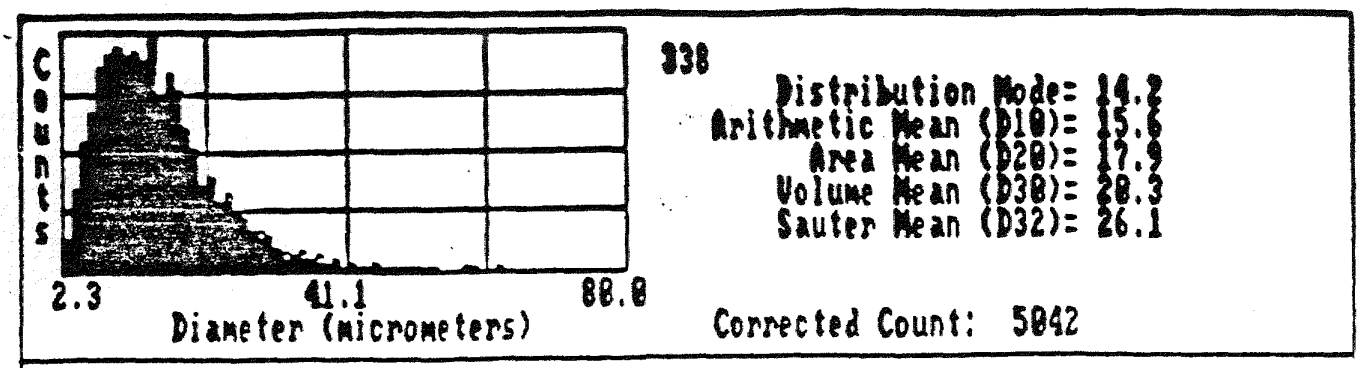

r = 0 z = 25.4 mm

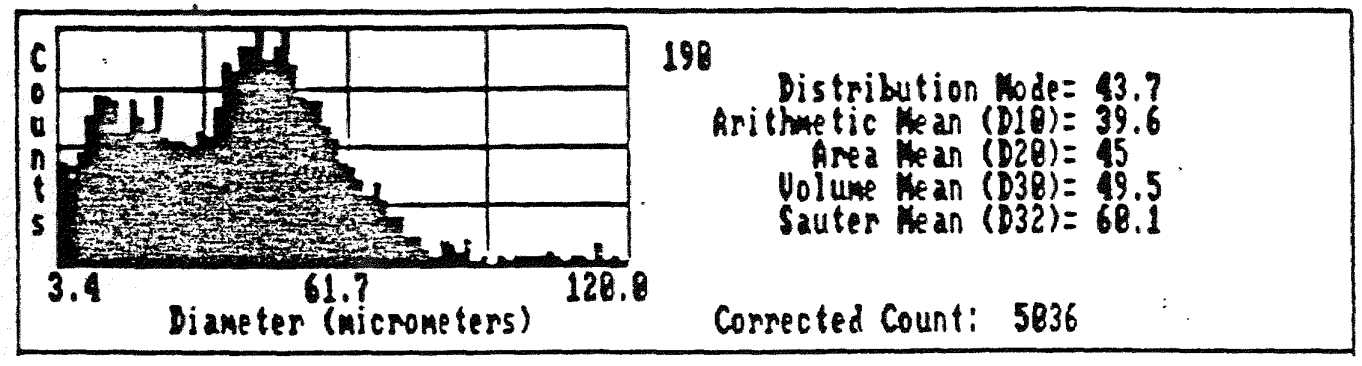

r = 15 mm z = 25.4 mm

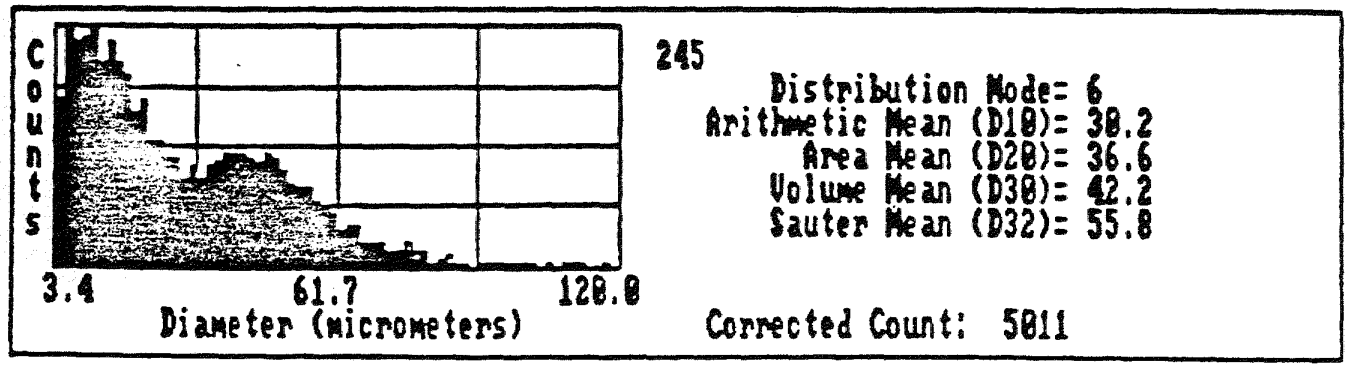

r = 17.8 mm z = 25.4 mm

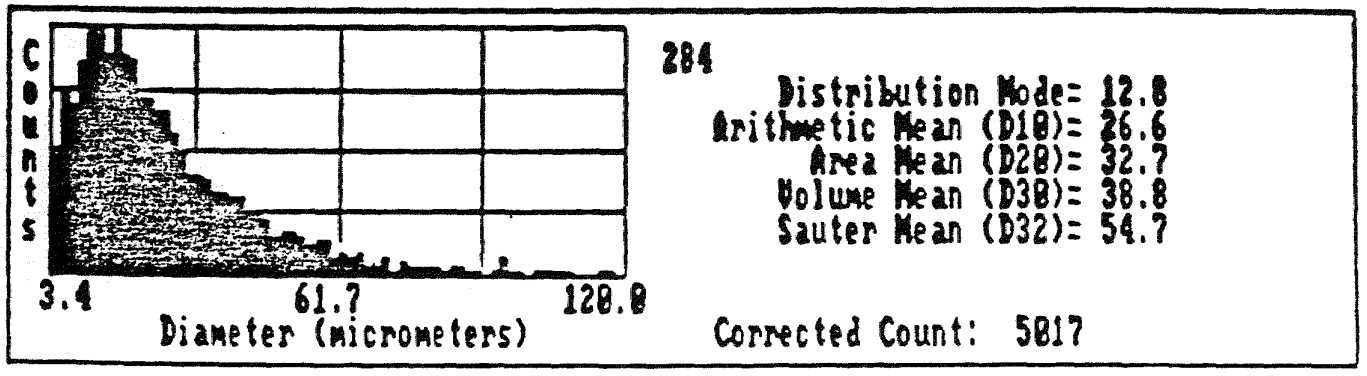

r = 25.4 mm z = 25.4 mm

FIGURE 16

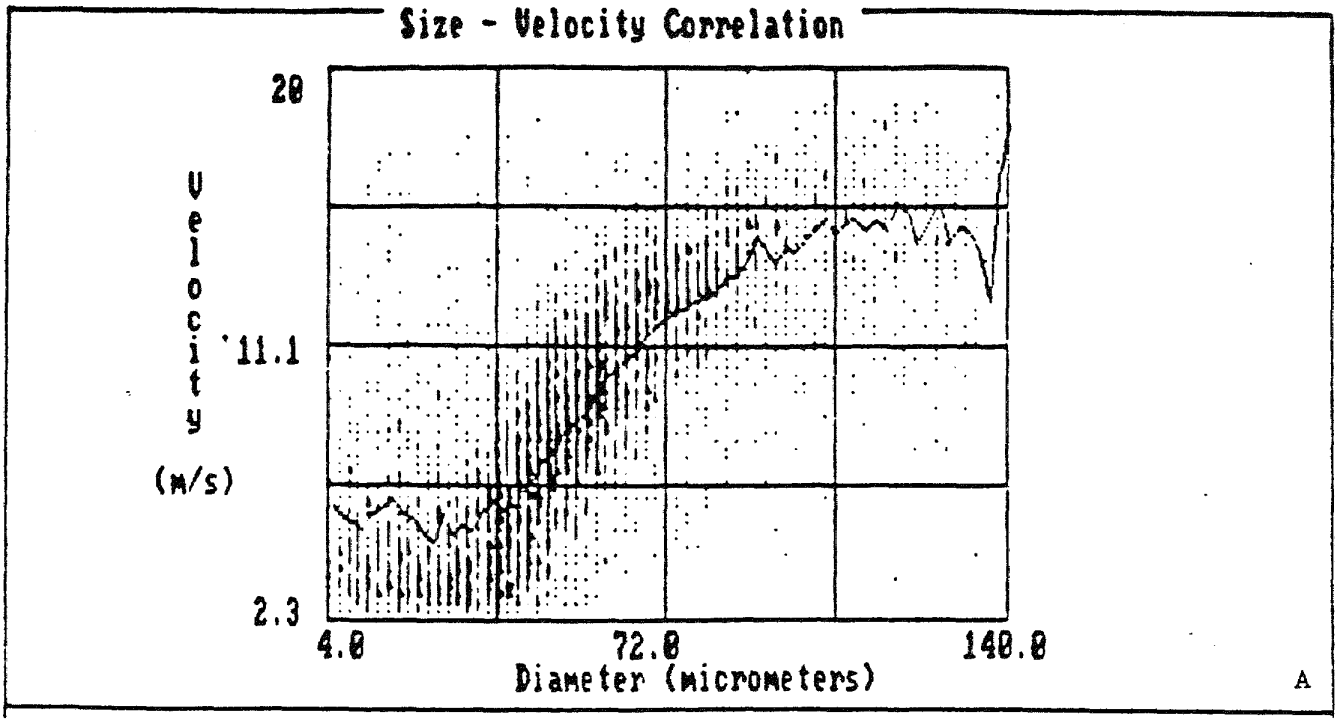

r = 15 mm z = 25.4 mm

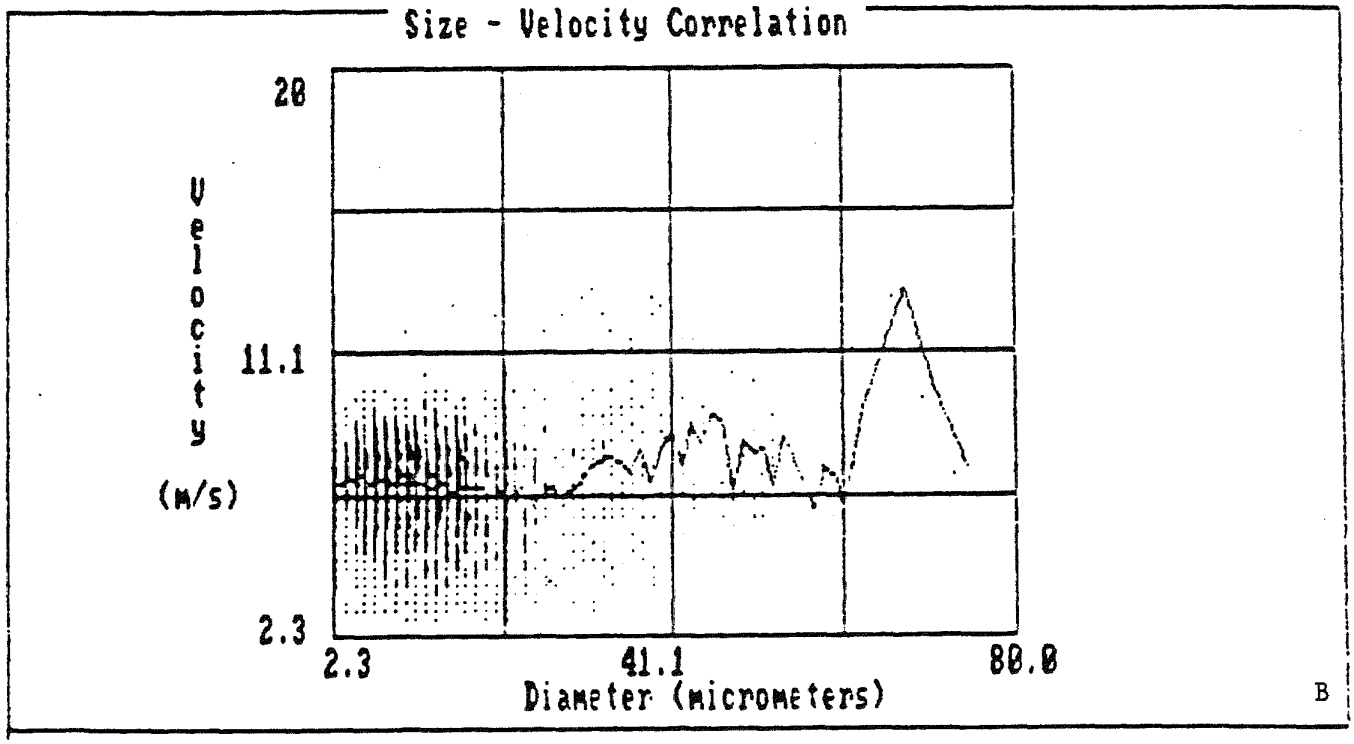

r = 0 z = 25.4 mm

FIGURE 17

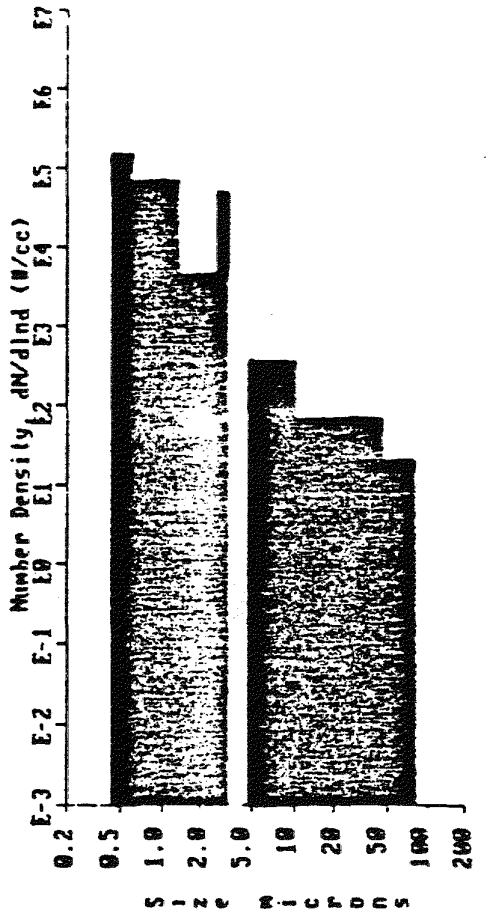

r = 38.1 mm z = 76.2 mm

FIGURE 18